to the other curve. We see that *the two curves represent the two stable states of a bistable system.* (We can, in fact, liken bi-stability of a chemical reaction to supercooling wherein a liquid may be cooled below the freezing point without solidifying). It may be emphasized that the two states are not in equilibrium states in the thermodynamic sense. They are in *steady states* which are far away from the equilibrium. The concentrations of X and Y are maintained as a result of the reactants continuously flowing into and of the products flowing out of the reactor.)

The presence of third intermediate Z, capable of reacting with both X and Y, causes dramatic change. Suppose that in the absence of Z, the flows of the reacting species correspond to the stable state *c* on the upper curve (Fig. 14*b*). When, however, Z reacts with Y to produce X, Y decreases and X increases so that the state of the system moves towards the right along the curve until a sudden transition occurs to the lower curve. Therefore, Z reacts with X producing Y, with the result that the state of the system moves towards the left along the lower curve until another sudden transition occurs to the upper curve when the process starts again. The result is a periodic surge and depletion of concentration of Y, arising out of a sudden leaping from one stable state to another in the bistability occurring in an oscillatory reaction (Fig. 15).

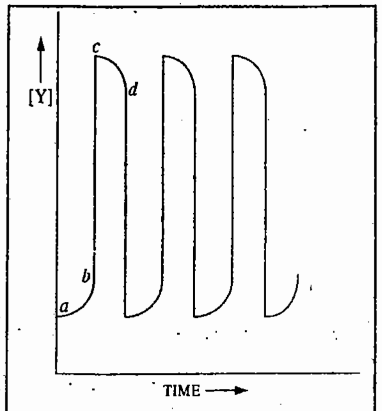

Fig. 15. Periodic surge and depletion of concentration in a bi-stable system.

Considerable research is going on to discover oscillatory reactions of industrial importance. The rhythm of the heartbeat is maintained by oscillatory reactions.

I. Review Questions

1. Illustrate the lowering of Gibbs free energy of activation of a reaction by a catalyst. Discuss carefully the general characteristics of catalytic reactions.
2. Discuss the kinetics of an acid–base catalyzed reaction.
3. Discuss the mechanism and kinetics of enzyme–catalyzed reactions.
4. The following mechanism has been proposed for enzyme catalysis :

$$E + S \underset{k_{-1}}{\overset{k_1}{\longrightarrow}} ES, \quad ES \xrightarrow{k_2} P + E$$

   Using steady state approximation for [ES], show that the reaction rate is given by

$$r = k_2[E]_0[S]/(K_m + [S])$$

   where the symbols have their usual meanings. Discuss the rate when $K_m >> [S]$ and $K_m >> [S]$.
5. Consider the following mechanism for an enzyme–catalyzed reaction :

$$E + S \underset{k_{-1}}{\overset{k_1}{\longrightarrow}} ES; \quad ES \xrightarrow{k_2} EP; \quad EP \xrightarrow{k_3} E + P$$

   where the symbols have their usual meanings and EP represents the complex formed between the enzyme and the product. Using steady state approximation, show that

$$r = \frac{k_2[E]_0[S]}{(k_{-1} + k_2)/k_1 + (1 + k_2/k_3)[S]}$$

6. Discuss the kinetics of (*i*) unimolecular surface reactions (*ii*) bimolecular surface reactions.
7. Discuss the *p*H-dependence of rate constants of catalyzed reactions.
8. What are oscillatory reactions ? Discuss in detail their mechanism.

CHAPTER 31

THE SOLID STATE

Solids are characterised by incompressibility, rigidity and mechanical strength. This indicates that the molecules, atoms or ions that make up a solid are closely packed. They are held together by strong cohesive forces and cannot move at random. Thus, in solids we have well ordered molecular, atomic or ionic arrangement.

Some solids, like sodium chloride, sulphur and sugar, besides being incompressible and rigid, have also characteristic geometrical forms. Such substances are said to be crystalline solids. The X-ray diffraction studies reveal that their ultimate particles (*viz.*, molecules, atoms or ions) are arranged in a definite pattern throughout the entire three-dimensional network of a crystal. This definite and ordered arrangement of molecules, atoms or ions (as the case may be) extends over a large distance. This is termed as **long range order**. There is another category of solids such as glass, rubber and plastics, which possess properties of incompressibility and rigidity to a certain extent but they do not have definite geometrical forms. Such substances are called **amorphous solids.**

Difference between Crystalline and Amorphous Solids. Crystalline and amorphous solids differ from one another in the following respects.

1. **Characteristic Geometry.** A crystalline solid has a definite and regular geometry due to definite and orderly arrangement of molecules or atoms or ions in three-dimensional space. An amorphous solid, on the other hand, does not have any pattern of arrangement of molecules or atoms and, therefore, does not have any definite geometrical shape. It has been found that even if some orderly arrangement of molecules or atoms exits in a few amorphous solids, it does not extend more than a few Angstrom units. Thus, unlike crystalline solids, amorphous solids do not have a long range order.

2. **Melting Points.** Consider a molecular solid which is being heated. With increase in temperature its molecular vibrations increase and ultimately become so great that molecules break away from their fixed positions. They now begin to move more freely and have rotational motion as well. The solid now changes into liquid state. The temperature at which this occurs is known as the **melting point.**

A crystalline substance has a sharp melting point, *i.e.*, it changes abruptly into liquid state. An amorphous substance, on the contrary, does not have a sharp melting point. For example, if glass is heated gradually, it softens and starts to flow without undergoing a definite and abrupt change. The amorphous solids are, therefore, regarded as 'liquids at all temperatures'. There is some justification for this view because it is known from X-ray examination that amorphous substances do not have well ordered molecular or atomic arrangements. Strictly speaking, solid state refers only to crystalline state, *i.e.*, only a crystalline material can be considered to be a true solid.

3. **Isotropy and Anisotropy.** Amorphous substances differ from crystalline solids and resemble liquids in another important respect. Their properties such as electrical conductivity, thermal conductivity, mechanical strength and refractive index are the same in all directions. Amorphous substances are, therefore, said to be **isotropic.** Liquids and gases are also isotropic. Crystalline

solids, on the other hand, are anisotropic, *i.e.*, their physical properties are different in different directions. For example, the velocity of light passing through a crystal varies with the direction in which it is measured. Thus, a ray of light entering such a crystal may split up into two components each following a different velocity. This phenomenon is known as **double refraction.** Thus, anisotropy itself is a strong evidence for the existence of ordered molecular or atomic or ionic arrangement in such materials. This can be shown on reference to Fig. 1 in which a simple two-dimensional arrangement of only two different kinds of atoms is depicted. If the properties are measured along the direction indicated by the slanting line CD, they will be different from those measured in the direction indicated by the vertical line AB. The reason is that while in the first case, each row is made up of alternate types of atoms, in the second case, each row is made up of one type of atoms only. In amorphous solids, atoms or molecules are arranged at random and in a disorderly manner and, therefore, all directions are identical and all properties are alike in all directions.

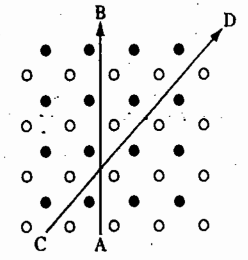

Fig. 1. Anisotropic behaviour of crystals.

Size and Shape of Crystals. Several naturally occurring solids have definite crystalline shapes which can be recognised easily. There are many other solid materials which occur as powders or agglomerates of fine particles and appear to be amorphous. But when an individual particle is examined under a microscope, it is also seen to have a definite crystalline shape. Such solids, in which the crystals are so small that they can be recognised only under a powerful microscope, are said to be **microcrystalline.** The size of a crystal depends on the rate at which it is formed : the slower the rate, the bigger the crystal. This is because time is needed by the atoms or ions or molecules to find their proper positions in the crystal structure. Thus, large transparent crystals of sodium chloride, silver nitrate, lithium chloride, etc., can be prepared by melting these salts and allowing them to cool very slowly at a uniform rate. It is for this reason that crystals of most of the minerals formed by geological processes in nature are often very large.

Interfacial Angles. Crystals are bound by plane faces. The angle between any two faces is called an **interfacial angle.** Although the size of the faces or even shapes of the crystals of one and the same substance may vary widely with conditions of formation, etc., yet the interfacial angles between any two corresponding faces of the crystal remain invariably the same throughout. This is illustrated in Fig. 2. Although the external shape is different yet the interfacial angles are the same. The measurement of interfacial angles in crystals is, therefore, important in the study of crystals. The subject is known as crystallography.

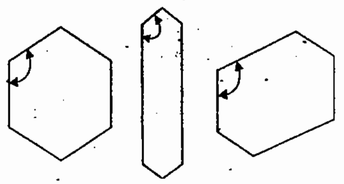

Fig. 2. Interfacial angles in a crystal.

SYMMETRY IN CRYSTAL SYSTEMS

Besides the interfacial angles, another important property of crystals is their symmetry. There are various types of symmetry, only three of which will be described here. These are : *(i)* Plane of Symmetry *(ii)* Axis of Symmetry and *(iii)* Centre of Symmetry.

Plane of Symmetry. When an imaginary plane can divide a crystal into two parts such that one is the exact mirror image of the other, the crystal is said to have a **plane of symmetry.**

Axis of Symmetry. An **axis of symmetry** is a line about which the crystal may be rotated such that it presents the same or similar appearance more than once during the complete revolution.

For example, in the case of a cube, an axis passing perpendicularly through the centre is such that when the cube is rotated it presents similar appearance in three rotations of 90° each and the same appearance after the fourth rotation. Such an axis is called a **four-fold** or a **tetrad axis** (Fig. 3*a*). If the same or similar appearance is repeated after an angle of 180°, the axis is called a **two-fold** or a **diad axis** (Fig. 3*b*). In the same way, if the same or similar appearance is repeated after an angle of 120°, the axis is called a **three-fold** or **triad axis** (Fig. 3*c*). If the same or similar appearance is repeated after an angle of 60°, as in the case of a hexagonal crystal, the axis is called a **six-fold** or **hexad axis** (Fig. 3*d*). In general, if the same or similar appearance of a crystal is repeated on rotation through an angle of 360°/n, around an imaginary axis, the axis is called an **n-fold axis.** A crystal can have only 2-fold, 3-fold, 4-fold and 6-fold axes of rotation. The angle through which the crystal will have to be rotated to get the same or similar appearance, evidently, will be 180°, 120°, 90° and 60°, respectively.

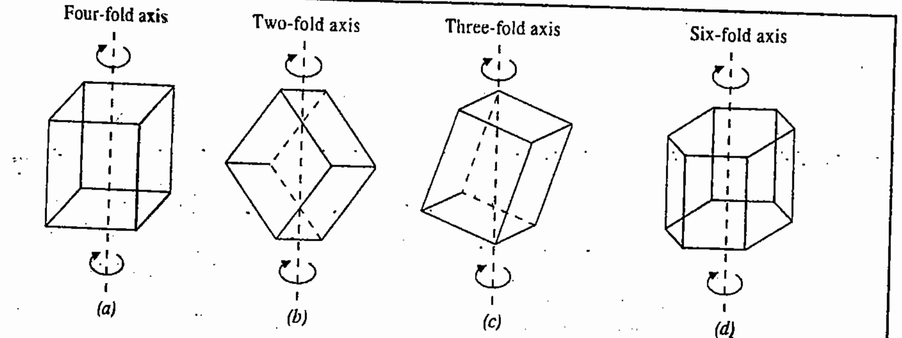

Fig. 3. Various axes of symmetry.

Centre of Symmetry. Centre of symmetry of a crystal is such a point that any line drawn through it intersects the surface of the crystal at equal distances in both directions.

It may be pointed out that a crystal may have any number of planes or axes of symmetry but it has only **one** centre of symmetry.

Elements of Symmetry of a Crystal. As mentioned above, there are different types of symmetries which are possible in a crystal. A crystal may have different numbers of each type of symmetry. The total number of **planes, axes** and **centre** of symmetries possessed by a crystal is termed as **elements of symmetry** of the crystal. To explain this term further, we may consider the elements of symmetry possessed by a **cubic crystal,** such as NaCl crystal. A cubic crystal possesses **a total of 23 elements of symmetry,** as will be clear from the discussion given below. These elements of symmetry are :

a. Rectangular planes of symmetry. One rectangular plane of symmetry is shown in Fig. 4*a*. There will be two more such planes, each of which will be at right angles to the plane shown in the figure. Thus, there are 3 rectangular planes of symmetry in all.

b. Diagonal planes of symmetry. One plane passing

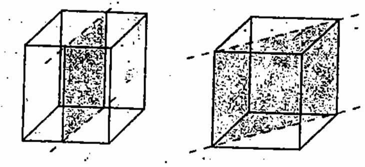

Rectangular plane of symmetry
(a)

Diagonal plane of symmetry
(b)

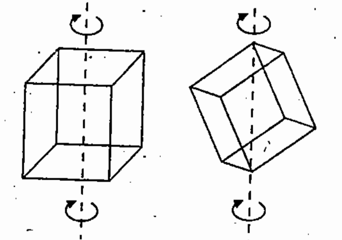

Axis of four-fold symmetry
(c)

Axis of three-fold symmetry
(d)

diagonally through the cube is shown in Fig. 4*b*. There can be a total of 6 such planes passing diagonally through the cube, as a little reflection will show.

c. Axes of four-fold symmetry. One of the four-fold axes is shown in Fig. 4*c*. Evidently, there can be a total of 3 such four-fold axes at right angles to one another.

d. Axes of three-fold symmetry. One such axis passing through opposite corners is shown in Fig. 4*d*. There can be a total of 4 such three-fold axes.

e. Axes of two-fold symmetry. One such axis emerging from opposite edges is shown in Fig. 4*e*. There are, evidently, 6 such axes of two-fold symmetry.

f. Centre of symmetry. There is only one centre of symmetry lying at the centre of the cube (Fig. 4*f*).

Thus, the number of symmetry elements of various types in a cubic crystal are :

Planes of symmetry = 3 + 6 = 9 elements
Axes of symmetry = 3 + 4 + 6 = 13 elements
Centre of symmetry = 1
Total number of symmetry elements = 23

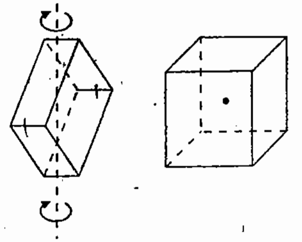

Axis of two-fold symmetry (*e*) Centre of symmetry (*f*)

Fig. 4. Various elements of symmetry in a cubic crystal.

Point Groups and Space Groups

It can be shown from geometrical considerations that, theoretically, there can be 32 different combinations of elements of symmetry of a crystal. These are called 32 point groups or 32 crystal systems. Some of the systems, however, have been grouped together so that we have only seven different categories, known as the seven basic crystal systems. These are cubic, orthorhombic, tetragonal, monoclinic, triclinic, hexagonal and rhombohedral or trigonal.

These systems together with the maximum numbers of planes of symmetry and axes of symmetry and their examples are given in Table 1.

TABLE 1
Crystal Systems and their Maximum Symmetry Elements

Sr.	System	Maximum Symmetry Elements	Examples
1.	Cubic or Regular	Nine planes of symmetry Thirteen axes of symmetry	NaCl, KCl, CaF_2, ZnS, Cu_2O. Diamond, Alums, Pb, Ag, Au.
2.	Orthorhombic	Three planes of symmetry Three axes of symmetry	KNO_3, K_2SO_4, $BaSO_4$ Mg_2SiO_4, Rhombic sulphur
3.	Tetragonal	Five planes of symmetry Five axes of symmetry	SnO_2, TiO_2, $ZrSiO_4$, KH_2PO_4 $PbWO_4$, Sn
4.	Monoclinic	One plane of symmetry One axis of symmetry	$Na_2SO_4.10H_2O$, $Na_2B_4O_7.10H_2O$, $CaSO_4.2H_2O$, Monoclinic sulphur
5.	Triclinic	No plane of symmetry No axis of symmetry	$CuSO_4.5H_2O$, $K_2Cr_2O_7$, H_3BO_3
6.	Hexagonal	Seven planes of symmetry Seven axes of symmetry	ZnO, CdS, HgS, Graphite Ice, PbI_2, Beryl, Mg, Zn, Cd
7.	Rhombohedral or Trigonal	Seven planes of symmetry Seven axes of symmetry	$NaNO_3$, ICl, Calcite, Magnesite Quartz, As, Sb, Bi

The 32 point groups can further produce 230 space groups, as discussed in Chapter 3 on Group theory.

Space Lattice and Unit Cell. A space lattice is an array of points showing how molecules, atoms or ions are arranged at different sites in three-dimensional space. An array of points in a three-dimensional space lattice is shown in Fig. 5. Each point represents a molecule, an atom or an ion or a group of any of these constituents.

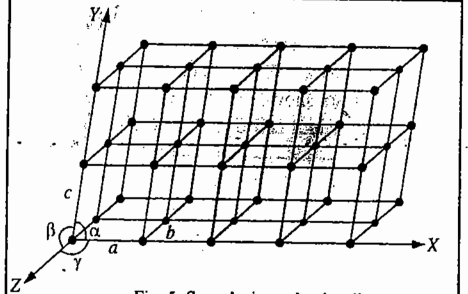

Fig. 5. Space lattice and unit cell.

The lattice points can be broken up into a number of unit cells. This is done by connecting the points by a regular network of lines, as shown in the figure. A **unit cell** *is the smallest repeating unit in space lattice which when repeated over and over again results in a crystal of the given substance.* Thus, space lattice of a crystal has been likened to a wall paper on which a single pattern is continuously repeated. Just as a pattern on the wall paper is repeated again and again, similarly, a unit cell (representing a definite pattern) is repeated again and again to build up a crystal. The only difference is that while wall paper is in two dimensions, space lattice of a crystal is in three dimensions. The unit cell, in fact, is the smallest sample that represents the picture of the entire crystal. The crystal may be considered to consist of infinite number of unit cells. Each unit cell in a three-dimensional space has, evidently, three vectors, *a*, *b* and *c*, as shown in Fig. 5.

It may be noted that these are the *points* and *not the lines* which constitute the space lattice. The lines joining the points are drawn simply to represent three axes by means of which the relative positions of the points can be described. For example, in Fig. 5, three imaginary axes, *OX*, *OY* and *OZ*, which may be used to represent the unit cell, have been shown. In order to describe a unit cell, we should know the distances *a*, *b* and *c* which give the lengths of the edges of the unit cell and the angles α, β and γ, which give the angles between the three imaginary axes, as shown. Knowing the unit cell dimensions, the theoretical density ρ of a crystal can be calculated from the relation

$$\rho = nM/(N_A V) \qquad ...(1)$$

where *n* is the number of molecules or atoms or ions in the unit cell ; *M* is the molar mass of the substance and *V* is the volume of the unit cell.

Bravais Lattices

The French crystallographer Auguste Bravais in 1848 showed from geometrical considerations that there can be only 14 different ways in which similar points can be arranged in a three-dimensional space. Thus, the total number of space lattices belonging to all the seven basic crystal systems put together is only 14, as given in column 2 of Table 2.

The crystals belonging to the cubic system have three kinds of Bravais lattices depending upon the shape of the unit cell. These are :

1. The **simple** or **primitive cubic lattice (P)** in which there are points only at the corners of each unit cell (Fig. 6*a*).
2. The **face-centred cubic lattice (F)** in which there are points at the corners as well as at the centre of each of the six faces of the cube (Fig. 6*b*).
3. The **body-centred cubic lattice (I)** in which there are points

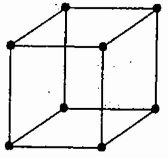

Fig. 6(*a*) Simple or primitive cubic lattice (P)

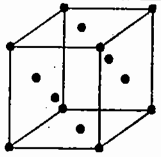

Fig. 6(*b*) Face-centred cubic lattice (F)

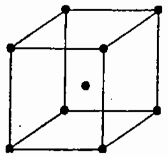

Fig. 6(*c*) Body-centred cubic lattice (I) at the corners as well as in the body centre of each cube (Fig. 6*c*).

The Bravais space lattices associated with various crystal systems are shown in Figs. 7*a*, 7*b*, 7*c* and 7*d*. The parameters of unit cell, *i.e.*, the cell dimensions *a*, *b*, *c* and the interfacial angles α, β and γ are also shown in each case. The actual lattice in a crystal of a given kind consists of a repetition of a unit cell of that kind all over in three-dimensional space.

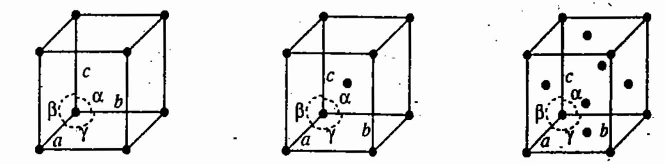

Simple or Primitive (P) Body-centred (I) Face-centred (F)

Fig. 7*a*. Cubic Space Lattices

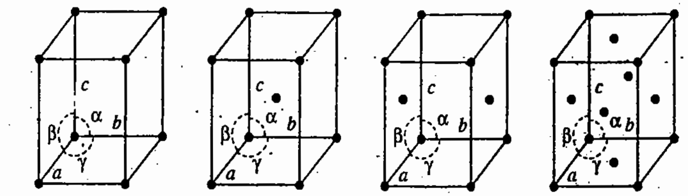

Simple or Primitive (P) Body-centred (I) End-centred (C) Face-centred (F)

Fig. 7*b*. Orthorhombic Space Lattices

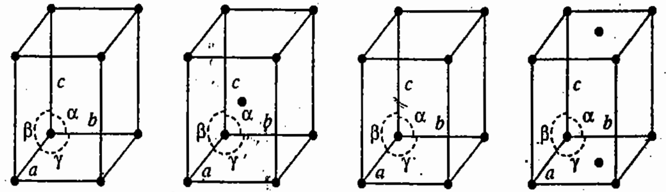

Simple (P) Body-centred (I) Simple (P) End-centred (C)

Fig. 7*c*. Tetragonal and Monoclinic Space Lattices

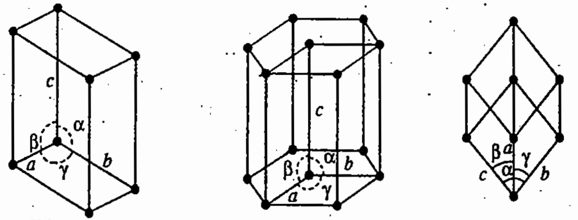

Triclinic (P) Hexagonal (P) Rhombohedral or Trigonal (P)

Fig. 7*d*. Triclinic, Hexagonal and Rhombohedral Space Lattices

Seven Crystal Systems. The crystallographers have been able to divide 32 point groups and 14 space lattices into seven crystal systems. Some detailed descriptions of these seven crystal systems are given in Table 2.

TABLE 2
Seven Crystal Systems

Crystal System	Bravais Lattices	Minimum symmetry Elements	Parameters of Unit Cell	
			Cell Dimensions	Interfacial Angles
1. Cubic	Primitive, Face-centred, Body-centred = 3	Four 3-fold axes : Three 4-fold axes	$a=b=c$	$\alpha=\beta=\gamma=90°$
2. Orthorhombic	Primitive, Face-centred, Body-centred, End-centred = 4	Three mutually perpendicular 2-fold axes	$a\neq b\neq c$	$\alpha=\beta=\gamma=90°$
3. Tetragonal	Primitive, Body-centred = 2	One 4-fold axis	$a=b\neq c$	$\alpha=\beta=\gamma=90°$
4. Monoclinic	Primitive, End-centred = 2	One 2-fold axis	$a\neq b\neq c$	$=\gamma=90°, \beta\neq 90°$
5. Triclinic	Primitive = 1	One 1-fold axis	$a\neq b\neq c$	$\alpha\neq\beta\neq\gamma\neq 90°$
6. Hexagonal	Primitive = 1	One 6-fold axis	$a=b\neq c$	$\alpha=\beta=90°, \gamma=120°$
7. Rhombohedral or Trigonal	Primitive = 1	One 3-fold axis	$a=b=c$	$\alpha=\gamma=\beta\neq 90°$

The first column gives the name of the crystal system. The second column gives the number and types of space lattices present in the given crystal system. The third column contains information with regard to minimum symmetry elements of each system. These are the absolutely essential symmetry requirements of a given crystal system. A crystal belonging to that system may have more symmetry elements but it cannot have less. The unit cell parameters, *viz.*, the cell dimensions *a*, *b* and *c* and the interfacial angles α, β and γ between the three imaginary axes are given in the last column.

Example 1. A metallic element exists as a cubic lattice. Each edge of the unit cell is 2·88 Å. The density of the metal is 7·20 g cm^{-3}. How many unit cells there will be in 100 g of the metal ?

Solution : Volume of the unit cell $= (2{\cdot}88\ \text{Å})^3 = 23{\cdot}9\times10^{-30}\ \text{m}^3$

$$\text{Volume of 100 g of the metal} = \frac{m}{\rho} = \frac{0{\cdot}1\ \text{kg}}{7{\cdot}20\times10^3\ \text{kg m}^{-3}} = 13{\cdot}9\times10^{-6}\ \text{m}^3$$

$$\text{Number of unit cells in this volume} = \frac{13{\cdot}9\times10^{-6}\ \text{m}^3}{23{\cdot}9\times10^{-30}\ \text{m}^3} = \mathbf{5{\cdot}82\times10^{23}}$$

Example 2. Iron (II) oxide, FeO, crystal has a cubic structure and each edge of the unit cell is 5·0 Å. Taking density of the oxide as 4·0 g cm^{-3}, calculate the number of Fe^{2+} and O^{2-} ions present in each unit cell.

Solution : Volume of the unit cell $= (5\times10^{-10}\ \text{m})^3 = 1{\cdot}25\times10^{-28}\ \text{m}^3$

Density of FeO $= 4{\cdot}0\times10^3\ \text{kg cm}^{-3}$

∴ Mass of the unit cell $= 1{\cdot}25\times10^{-28}\ \text{m}^3\times4{\cdot}0\times10^3\ \text{kg m}^{-3} = 5{\cdot}0\times10^{-25}\ \text{kg}$

$$\text{Mass of one molecule of FeO} = \frac{\text{Molar mass}}{\text{Avogadro's number}} = \frac{72\times10^3\ \text{kg mol}^{-1}}{6{\cdot}022\times10^{23}\ \text{mol}^{-1}}$$

$$= 1{\cdot}195\times10^{-25}\ \text{kg}$$

$$\therefore\ \text{Number of FeO molecules per unit cell} = \frac{5{\cdot}0\times10^{-25}\ \text{kg}}{1{\cdot}195\times10^{-25}\ \text{kg}} = 4{\cdot}19 \approx 4$$

Thus, there are **four Fe^{2+}** ions and **four O^{2-}** ions in each unit cell.

Example 3. Calculate the number of atoms contained within *(i)* a primitive cubic unit cell *(ii)* a body-centred cubic (b.c.c.) unit cell *(iii)* a face-centred cubic (f.c.c.) unit cell and *(iv)* the unit cell for the diamond lattice.

Solution : *(i)* The primitive cubic unit cell consists of one atom at each of the 8 corners. Each atom is thus shared by 8 unit cells. Hence, $n = 8\times(1/8) = 1$.

(ii) The b.c.c. unit cell consists of 8 atoms at the 8 corners and one atom at the centre. At each corner only 1/8th of the atom is within the unit cell. Thus, the contribution of the 8 corners is $8\times(1/8)=1$ while that of the body-centred atom is 1. Hence, $n = 1+1 = 2$.

(iii) The 8 atoms at the corners contribute $8\times(1/8) = 1$. There is one atom at each of the 6 faces, which is shared by 2 unit cells each. Therefore, the contribution of 6 face-centred atoms $= 6\times(1/2) = 3$. Hence, $n = 1+3 = 4$.

(iv) If we consider the unit cell of a diamond lattice, we find that there are 8 atoms on the 8 corners, each shared by 8 unit cells. Also, there are 6 atoms on the faces, each shared by 2 unit cells. In addition, there are 4 atoms inside the unit cell. Hence, $n = 8\times(1/8) + 6\times(1/2) + 4 = 8$.

Example 4. Calculate the coordination number (C.N.) of an atom in *(i)* a primitive cubic unit cell *(ii)* a body-centred cubic unit cell and *(iii)* a face-centred cubic unit cell.

Solution : *(i)* A little consideration shows that in a primitive cubic unit cell, each atom has 6 equally-spaced nearest neighbour atoms. Thus, C.N. = 6.

(ii) Considering the atom at the centre of the unit cell, we find that it is surrounded by 8 nearest neighbour atoms situated at the corners of the cube. Thus, C.N. = 8.

(iii) C.N. for a face-centred atom in an f.c.c. unit cell is, evidently, equal to **12**.

Example 5. At room temperature, pollonium crystallizes in primitive cubic unit cell. If $a = 3{\cdot}36$ Å, calculate the theoretical density of pollonium. Molar mass M of pollonium = 209 g mol^{-1}.

Solution : A primitive cubic unit cell contains atoms only at the 8 corners with each corner contributing 1/8th of an atom. Hence, $n = 8\times(1/8) = 1$.

$$\text{Volume, } V = a^3 = (3{\cdot}36\ \text{Å})^3 = (3{\cdot}36\times10^{-10}\ \text{m})^3$$

$$\text{From Eq. 1, } \rho = \frac{nM}{N_A V} = \frac{(1)(209\times 10^{-3}\ \text{kg mol}^{-1})}{(6{\cdot}022\times10^{23}\ \text{mol}^{-1})(3{\cdot}36\times10^{-10}\ \text{m})^3} = \mathbf{9{\cdot}15\times10^3\ kg\ m^{-3}}$$

Example 6. At room temperature, sodium crystallizes in a body-centred cubic cell with a = 4·24 Å. Calculate the theoretical density of sodium. Molar mass M of sodium = 23·0 g mol^{-1}.

Solution : As shown in Example 3, the value of n for a b.c.c. unit cell is 2.

$$\text{Volume, } V = (4{\cdot}24\ \text{Å})^3 = (4{\cdot}24\times10^{-10}\ \text{m})^3$$

$$\text{From Eq. 1, } \rho = \frac{nM}{N_A V} = \frac{2\times(23{\cdot}0\times10^{-3}\ \text{kg mol}^{-1})}{(6{\cdot}022\times10^{23}\ \text{mol}^{-1})(4{\cdot}24\times10^{-10}\ \text{m})^3} = \mathbf{1{\cdot}00\times10^3\ kg\ m^{-3}}$$

Example 7. Lithium borohydride, $LiBH_4$, crystallizes in an orthorhombic system with 4 molecules per unit cell. The unit cell dimensions are : $a = 6{\cdot}81$ Å, $b = 4{\cdot}43$ Å and $c = 7{\cdot}17$ Å. If the molar mass M of $LiBH_4$ is 21·76 g mol^{-1}, calculate the density of the crystal.

$$\textbf{Solution :}\quad \rho = \left(\frac{nM}{N_A V}\right) = \frac{4\times(21{\cdot}76\times10^{-3}\ \text{kg mol}^{-1})}{(6{\cdot}022\times10^{23}\ \text{mol}^{-1})(6{\cdot}81\times4{\cdot}43\times7{\cdot}17\times10^{-30}\ \text{m}^3)} = \mathbf{0{\cdot}668\times10^3\ kg\ m^{-3}}$$

Example 8. An organic compound crystallises in an orthorhombic system with two molecules per unit cell. The unit cell dimensions are 12·05, 15·05 and 2·69 Å. If the density of the crystal is 1·419 g cm^{-3}, calculate the molar mass of the organic compound.

Solution : From Eq. 1, $M = \rho N_A V/n$

$$= \frac{(1{\cdot}419\times10^3\ \text{kg m}^{-3})(6{\cdot}022\times10^{23}\ \text{mol}^{-1})(12{\cdot}05\times15{\cdot}05\times2{\cdot}69\times10^{-30}\ \text{m}^3)}{2} = \mathbf{0{\cdot}209\ kg\ mol^{-1}}$$

Example 9. Iron (α-Fe) crystallises in a b.c.c. system with $a = 2{\cdot}861$ Å. Molar mass M of iron is 55·85 g mol^{-1}. Calculate the density of iron.

$$\textbf{Solution : } \text{From Eq. 1, } \rho = \frac{nM}{N_A V} = \frac{2\times(55{\cdot}85\times10^{-3}\ \text{kg mol}^{-1})}{(6{\cdot}022\times10^{23}\ \text{mol}^{-1})(2{\cdot}861\times10^{-10}\ \text{cm})^3} = \mathbf{7{\cdot}92\times10^3\ kg\ m^{-3}}$$

Lattice Energy of an Ionic Crystal. It is defined as the amount of energy released when cations and anions in their gaseous state are brought together from infinite separation to form a crystal.

$$M^+(g) + X^-(g) \xrightarrow{-U} MX(s)\ ;\ U = \text{lattice energy}$$

The theoretical treatment of ionic lattice energy was given by **M. Born** and **A. Lande'**. This treatment has been discussed below.

Consider the potential energy of an ion pair, M^+,X^- in a crystal separated by a distance r. The coulombic electrostatic energy of attraction is given by

$$U_{\text{att}}(r) = \frac{z_+ z_- e^2}{4\pi\varepsilon_0 r} \qquad \text{...(2)}$$

Since z_- is negative, the electrostatic energy is negative (with respect to energy at infinite separation) and becomes increasingly so as the interionic distance decreases, as shown by the dotted line in **Fig. 8**. Note that the charge on the cation is z_+e and that on the anion is z_-e.

In a crystal lattice there are more interactions between the ions than the simple one in an isolated ion pair. Thus, in NaCl lattice, each sodium ion experiences attraction to the six nearest chloride ions, repulsions by the next twelve nearest sodium ions, attractions to the next eight chloride ions and repulsions by the next six sodium ions and so on. The summation of all these geometrical interactions is known as the **Madelung constant,** M. The energy of attraction in an ion pair in a crystal is thus given by

$$U_{\text{att}}(r) = \frac{M z_+ z_- e^2}{4\pi\varepsilon_0 r} \qquad \text{...(3)}$$

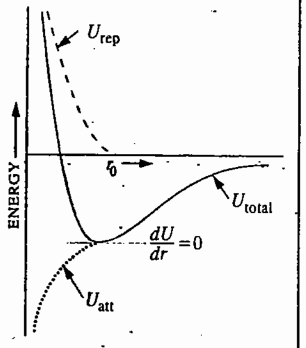

Fig. 8. Energy curves for an ion pair in an ionic solid.

The value of Madelung constant depends only on the geometry of the lattice and is independent of ionic radius and charge. Thus, the value of Madelung constant in NaCl lattice is given by

$$M = 6 - \frac{12}{\sqrt{2}} + \frac{8}{\sqrt{3}} - \frac{6}{\sqrt{4}} + \ldots. \qquad \text{...(4)}$$

A stable lattice can result only if there is also repulsion energy to balance the attractive coulombic energy. The attractive energy becomes infinite at infinitesimally small distances. However, ions are not point charges but consist of electron charge-clouds which repel each other at very close distances. This repulsion is shown by the broken line in Fig. 8. It is negligible at large distances but increases very rapidly as the ions approach each other closely. According to Born, the repulsive energy is given by

$$U_{\text{rep}}(r) = B/r^n \qquad \text{...(5)}$$

where B is a constant. Experimentally, the Born exponent n can be determined from the compressibility data because the latter measure the resistance which the ions exhibit when forced to approach each other very closely.

Thus, for a crystal lattice consisting of Avogadro's number of ions, the total energy is given by

$$U_{\text{total}}(r) = U_{\text{att}}(r) + U_{\text{rep}}(r) = \frac{MN_A z_+ z_- e^2}{4\pi\varepsilon_0 r} + \frac{N_A B}{r^n} \qquad \text{...(6)}$$

The total energy is shown by the solid line in Fig. 8. At the minimum in the curve, corresponding to the equilibrium lattice configuration, $(r = r_0)$

$$\left(\frac{dU}{dr}\right)_{r=r_0} = 0 = -\frac{MN_A z_+ z_- e^2}{4\pi\varepsilon_0 r_0^2} - n\frac{N_A B}{r_0^{n+1}} \qquad \text{...(7)}$$

In this lattice configuration, the attractive forces between the ions balance the repulsive forces. Let U_0 represent the energy at the equilibrium distance r_0. From Eq. 7,

$$B = -\frac{Mz_+z_-e^2 r_0^{n-1}}{4\pi\varepsilon_0 n} \qquad \ldots(8)$$

and

$$U_0 = \frac{MN_A z_+z_-e^2}{4\pi\varepsilon_0 r_0} - \frac{MN_A z_+z_-e^2}{4\pi\varepsilon_0 r_0 n} \qquad \ldots(9)$$

$$\frac{1}{4\pi\epsilon_0} = 9\times10^9\ \mathrm{Nm^2C^{-2}}$$

$$= \frac{MN_A z_+z_-e^2}{4\pi\varepsilon_0 r_0}\left(1-\frac{1}{n}\right) \qquad \ldots(10)$$

This is the **Born–Lande′ equation** for the lattice energy of an ionic crystal. The Born exponent n depends upon the type of the ion involved. Larger ions having relatively higher electron densities have larger values of n.

Example 10. Calculate the lattice energy of NaCl crystal from the following data :

$$M = 1{\cdot}7476\ ;\ r_0 = 2{\cdot}814\ \text{Å}\ ;\ n = 8$$

Solution : Substituting the given data and the values of the other constants in Eq. 10, we have

$$U_0 = \frac{(1{\cdot}7476)(6{\cdot}022\times10^{23}\ \mathrm{mol^{-1}})(1)(-1)(1{\cdot}602\times10^{-19}\ \mathrm{C})^2}{4(3{\cdot}1416)(8{\cdot}854\times10^{-12}\ \mathrm{C^2\ N^{-1}\ m^{-2}})(2{\cdot}814\times10^{-10}\ \mathrm{m})}\left(1-\frac{1}{8}\right)$$

$$= -\ 775\ \mathrm{kJ\ mol^{-1}}\ \text{(Experimental value} = -\ 770\ \mathrm{kJ\ mol^{-1}})$$

We see that the agreement of Born-Lande equation with experiment is satisfactory.

Substitution of the various constants in Eq. 10 gives the following equation :

$$U_0 = 1{\cdot}39\times10^5\left(\frac{z_+z_-M}{r_0\ (\mathrm{pm})}\right)\left(1-\frac{1}{n}\right)\ \mathrm{kJ\ mol^{-1}} \qquad \ldots(11)$$

Experimentally, the lattice enthalpy of an ionic compound can be determined by using the **Born–Haber cycle** which can be represented diagrammatically as shown below :

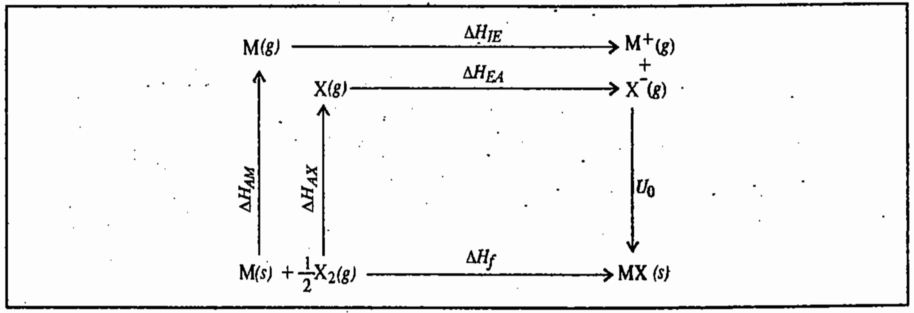

We find that

$$\Delta H_f = \Delta H_{AM} + \Delta H_{AX} + \Delta H_{IE} + \Delta H_{EA} + U_0$$

Here the terms ΔH_{AM} and ΔH_{AX} are the enthalpies of atomization of the metal and the non-metal, respectively ; ΔH_{IE} and ΔH_{EA} are the ionization energy of the metal and electron affinity of the non-metal, respectively.

Law of Rational Indices. This law states that the intercepts of any face of a crystal along the crystallographic axes are either equal to the unit intercepts (a, b, c) or some simple whole number multiples of them, *e.g.*, na, n′b, n″c, etc., where n, n′, n″, etc., are simple whole numbers.

Let *OX, OY* and *OZ* represent the three crystallographic axes and let *ABC* be a unit plane (Fig. 9). The unit intercepts will then be *a, b* and *c*. According to the above law, the intercepts of any face such as *KLM*, on the same three axes will be simple whole number multiples of *a, b* and *c*, respectively. As can be seen from the figure, the simple multiples in this case are 2, 2 and 3.

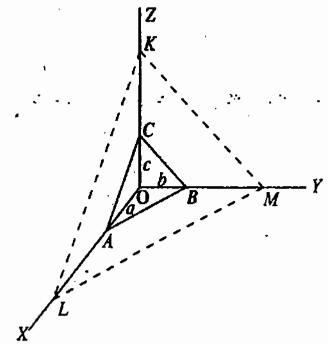

Fig. 9. Crystallographic axes and the law of rational indices.

Miller Indices. Miller indices are a set of integers (*h, k, l*) which are used to describe a given plane in a crystal. The miller indices of a face of a crystal are inversely proportional to the intercepts of that face on the various axes. The procedure for determining the Miller indices for a plane is as follows :

1. Prepare a three-column table with the unit cell axes at the tops of the columns.
2. Enter in each column the intercept (expressed as a multiple of *a, b* or *c*) of the plane with these axes.
3. Invert all numbers.
4. Clear fractions to obtain *h, k* and *l*.

Example 11. Calculate the Miller indices of crystal planes which cut through the crystal axes at *(i)* (2*a*, 3*b*, *c*) *(ii)* (*a*, *b*, *c*) *(iii)* (6*a*, 3*b*, 3*c*) and *(iv)* (2*a*, – 3*b*, – 3*c*).

Solution : Following the procedure given above, we prepare the table as follows :

(i) *a*	*b*	*c*	
2	3	1	intercepts
1/2	1/3	1	reciprocals
3	2	6	clear fractions

Hence, the Miller Indices are (326).

(ii) *a*	*b*	*c*	
1	1	1	intercepts
1	1	1	reciprocals
1	1	1	clear fractions

Hence, the Miller indices are (111).

(iii) *a*	*b*	*c*	
6	3	3	intercepts
1/6	1/3	1/3	reciprocals
1	2	2	clear fractions

Hence, the Miller indices are (122).

(iv) *a*	*b*	*c*	
2	– 3	– 3	intercepts
1/2	–1/3	–1/3	reciprocals
3	– 2	– 2	clear fractions

Hence, the Miller indices are $(3\bar{2}\bar{2})$

Note. The negative sign in the Miller indices is indicated by placing a bar on the integer. The Miller indices are enclosed within parentheses.

Interplanar Spacing in a Crystal System. It can be shown that in a crystal, the interplanar distance d_{hkl} is given by

$$1/(d_{hkl})^2 = (h/a)^2 + (k/b)^2 + (l/c)^2 \qquad \ldots(12)$$

where *h, k, l* are the Miller indices of the planes and *a, b, c* are the dimensions of the cell.

For a *cubic system*, $a = b = c$ so that from Eq. 12,

$$d_{hkl} = a/[h^2 + k^2 + l^2]^{1/2} \qquad \ldots(13)$$

For a *tetragonal system*, $a = b \neq c$ so that

$$1/(d_{hkl})^2 = (h^2 + k^2)/a^2 + l^2/c^2 \qquad \ldots(14)$$

For an *orthorhombic system*, $a \neq b \neq c$ so that

$$1/(d_{hkl})^2 = h^2/a^2 + k^2/b^2 + l^2/c^2 \qquad ...(15)$$

Example 12. The parameters of an orthorhombic unit cell are a=50 pm, b=100 pm, c=150 pm. Determine the spacing between the (123) planes.

Solution : For an orthorhombic unit cell, the interplanar distance, d_{hkl}, is given by

$$1/(d_{hkl})^2 = (h^2/a^2) + (k^2/b^2) + (l^2/c^2) \qquad ...(\text{Eq. } 15)$$

$$1/(d_{hkl})^2 = 1/(d_{123})^2 = (1/50 \text{ pm})^2 + (2/100 \text{ pm})^2 + (3/150 \text{ pm})^2 = 3(1/50 \text{ pm})^2$$

$$1/d_{123} = \sqrt{3}/50\text{pm} \text{ so that } d_{123} = 50\text{pm}/\sqrt{3} = \mathbf{29 \text{ pm}}$$

Example 13. The density of Li metal is 0·53 g cm^{-3} and the separation of the (100) planes of the metal is 350 pm. Determine whether the lattice is f.c.c. or b.c.c. M(Li)=6·941 g mol^{-1}.

Solution : Density, $\rho = 0{\cdot}53 \text{ g cm}^{-3} = 530 \text{ kg m}^{-3}$

For the cubic system, $d_{hkl} = a/[h^2 + k^2 + l^2]^{1/2}$

$$\therefore \quad d_{100} = \frac{a}{\sqrt{1^2+0^2+0^2}} = 350 \text{ pm} = 350 \times 10^{-12} \text{ m}$$

We know from Eq. 1, that

$$\rho = nM/(N_A V) = nM/(N_A a^3) \qquad (\because V = a^3)$$

$$\therefore \quad n = \frac{\rho N_A a^3}{M} = \frac{(530 \text{ kg m}^{-3})(6{\cdot}022 \times 10^{23} \text{ mol}^{-1})(350 \times 10^{-12} \text{m})^3}{6{\cdot}941 \times 10^{-3} \text{ kg mol}^{-1}} = \mathbf{1{\cdot}97 \approx 2}$$

As shown in Example 3, for an f.c.c. lattice, n=4 and for a b.c.c. lattice, n=2. **Hence, lithium has a *b.c.c. lattice*.**

X-RAY DIFFRACTION

The German physicist M. von Laue (1879–1960), in 1913, suggested the possibility of diffraction of X-rays by crystals. The reason for this suggestion was that the wave length of X-rays was of about the same order as the interatomic distances in a crystal. von Laue was awarded the 1914 Physics Nobel Prize for his discovery of diffraction of X-rays by crystals. In fact, W.H. Bragg succeeded in diffracting X-rays from sodium chloride crystal. This observation has proved to be highly useful in determining structures and dimensions of crystals as well as in the study of a number of properties of X-ray themselves.

The Bragg Equation. Bragg pointed out that unlike reflection of ordinary light, the reflection of X-rays can take place only at certain angles which are determined by the wave length of the X-rays and the distance between the planes in the crystal. The fundamental equation which gives a simple relation between the wave length of the X-rays, the interplanar distance in the crystal and the angle of reflection, is known as the Bragg equation.

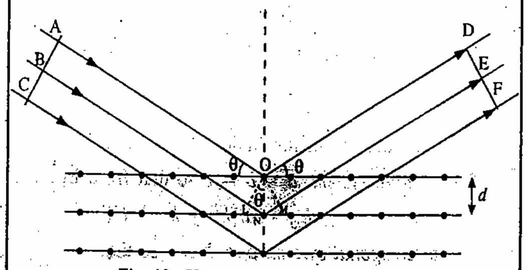

Fig. 10. X-ray reflections from a crystal.

Derivation of the Bragg Equation. Consider Fig. 10. The horizontal lines in this figure represent parallel planes in the crystal structure separated from one another by the distance d. Suppose a beam of X-rays falls on the crystal at **glancing angle** θ, as shown. Some of these rays will be reflected from the upper plane at the same angle θ while some others will be absorbed and get reflected from the successive layers, as shown. Let the planes ABC and DEF be drawn perpendicular to the incident and reflected beams, respectively. The waves reflected by different layer planes will be in phase with one another (i.e., will coincide with one another in the plane DEF) only if the difference in the path lengths of the waves reflected from the successive planes is equal to an integral number of wave lengths. Drawing OL and OM perpendicular to the incident and reflected beams, it will be seen that the difference in the path lengths (say, δ) of the waves reflected from the first two planes is given by

$$\delta = \text{LN} + \text{NM} \qquad ...(16)$$

This should be equal to a whole number multiple of wave length λ, *i.e.*,

$$\text{LN} + \text{NM} = n\lambda \qquad ...(17)$$

Since the triangles OLN and OMN are congruent, hence LN = NM.

$$\therefore \quad 2\text{LN} = n\lambda \quad \text{or} \quad 2d \sin\theta = n\lambda \qquad ...(18)$$

This is the Bragg equation. Knowing θ, n and λ, d can be calculated.

For a given set of lattice planes, d has a fixed value. Therefore, the possibility of getting maximum reflection (*i.e.*, the possibility of getting reflected waves in phase with one another) depends upon θ. If θ is increased gradually, a number of positions will be found at which the reflections will be maximum. At these positions, n will have values equal to 1, 2, 3, 4, 5, etc. Generally, in experiments on X-ray reflections, n is set as equal to 1. If λ is known, it is possible to determine d, the distance between atomic planes in the crystal by determining θ experimentally. On the other hand, if d is known, λ can be evaluated.

Experimental Methods. The X-ray diffraction techniques used in the study of crystals are of two types known as the rotating crystal technique and the powder technique. Both the techniques make use of the X-ray diffractometer, the setting of which for the former technique is shown in Fig. 11.

X-rays generated in the tube T are passed through a slit so as to obtain a narrow beam which is then allowed to strike a single crystal C mounted on the turn-table. The crystal is rotated gradually by means of the turn-table so as to increase the glancing angle at which the X-rays are incident at the exposed face of the crystal. The intensities of the reflected rays are measured on a recording device R, such as a photographic plate or an ionisation chamber. The angles for which reflections are maximum give the value of θ. The process is carried out for each plane of the crystal. The lowest angle at which the maximum reflection occurs corresponds to n=1. This is called the first order reflection. The next higher angle at which the maximum reflection occurs again, corresponds to n=2. This is the second order reflection, and so on.

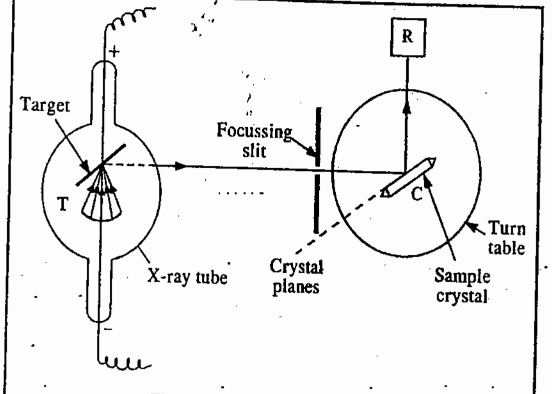

Fig. 11. An X-ray diffractometer.

The values of θ for the first order reflection from the three faces of sodium chloride crystal are found to be 5·9°, 8·4° and 5·2°, respectively. Applying the Bragg equation and knowing that n and λ are the same in each case, the distance d between successive planes in the three faces will be in the ratio of

$$1/\sin 5{\cdot}9° : 1/\sin 8{\cdot}4° : 1/\sin 5{\cdot}2° = 9{\cdot}61 : 6{\cdot}84 : 11{\cdot}04 = 1{\cdot}00 : 0{\cdot}70 : 1{\cdot}14$$

This ratio is very close to that expected to exist between spacings along the three planes of a face-centred cube. Thus, *sodium chloride has face-centred cubic structure.*

Powder Method : The Debye-Scherrer Method. The powder method is more widely used particularly for crystals with simple structures. The powder, in fact, consists of many small crystals which are oriented in all possible directions. As a result of this, X-rays are scattered from all sets of planes (*e.g.*, 100, 110, etc.). The scattered rays are detected by using an X-ray-sensitive film. The principle of the method is illustrated in Fig. 12. The substance to be examined is finely powdered and is kept in the form of a cylinder inside a thin glass tube. A narrow beam of X-rays is allowed to fall on the powder. The diffracted X-rays strike a strip of photographic film arranged in the form of a circular arc, as shown in the figure.

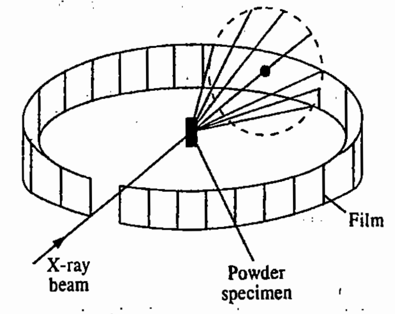

Fig. 12. The powder method for X-ray diffraction.

In this method, no rotation is necessary since the powder sample already contains microcrystals arranged in all possible orientations. Hence, a large number of them will have their lattice planes in correct positions for maximum X-ray reflection to occur. As a result of this we get lighted areas in the form of arcs of lines at different distances from the incident beam, as shown. These distances can be converted into scattering angles to be used in the Bragg equation for different planes of the crystal.

The British physicists W.H. Bragg (1862–1942) and his son W.L. Bragg (1890–1971) shared the 1915 Physics Nobel Prize for the analysis of crystal structure with X-rays. W.L. Bragg became at 25 the youngest Nobel Laureate in history. The Bragg equation is named after both the father and the son.

Example 14. KNO_3 crystallizes in orthorhombic system with the unit cell dimensions a=542 pm, b=917 pm and c=645 pm. Calculate the diffraction angles for first order X-ray reflections from (100), (010) and (111) planes using radiation with wave length=154·1 pm.

Solution : $2d_{hkl} \sin\theta = n\lambda$

For an orthorhombic system, we have

$$1/(d_{hkl})^2 = (h/a)^2 + (k/b)^2 + (l/c)^2 \qquad \text{...(Eq. 15)}$$

$$\therefore \quad 1/(d_{100})^2 = (1/542\text{ pm})^2 + (0/917\text{ pm})^2 + (0/645\text{ pm})^2 = (1/542\text{ pm})^2$$

$$\therefore \quad d_{100} = a = 542\text{ pm}$$

Similarly, $d_{010} = b = 917$ pm and $d_{111} = c = 378$ pm

For first order reflection, $n = 1$. Also $\lambda = 154{\cdot}1$ pm

$$\therefore \quad \sin\theta_{100} = \frac{\lambda}{2d_{100}} = \frac{154{\cdot}1\text{ pm}}{2 \times 542\text{ pm}} = 0{\cdot}142 \qquad \text{whence} \quad \theta_{100} = 8°10'$$

$$\sin\theta_{010} = \frac{\lambda}{2d_{010}} = \frac{154{\cdot}1\text{ pm}}{2 \times 917\text{ pm}} = 0{\cdot}084 \qquad \text{whence} \quad \theta_{010} = 4°\ 49'$$

$$\sin\theta_{111} = \frac{\lambda}{2d_{111}} = \frac{154{\cdot}1\text{ pm}}{2 \times 378\text{ pm}} = 0{\cdot}204 \qquad \text{whence} \quad \theta_{111} = 11°\ 46'$$

Example 15. $HgCl_2$ crystallizes in orthorhombic system. Using radiation with λ=154 pm, the (100), (010) and (001) reflections (first order) from $HgCl_2$ in an X-ray diffractometer occur at 7° 25′, 3° 28′ and 10° 23′, respectively. If the density of the crystal is 5·42 g cm^{-3}, calculate the dimensions of the unit cell and the number of $HgCl_2$ molecules in the unit cell. $M(HgCl_2)$=271·5 g mol^{-1}.

Solution : **Dimensions of the unit cell :** For first order reflections, n=1. Hence,

$$2\ d_{hkl} \sin\theta_{hkl} = \lambda \qquad \text{so that} \quad d_{hkl} = \lambda/2 \sin\theta_{hkl}$$

For the orthorhombic system,

$$1/(d_{hkl})^2 = (h/a)^2 + (k/b)^2 + (l/c)^2$$

$$1/(d_{100})^2 = (1/a)^2 + (0/b)^2 + (0/c)^2 = 1/a^2$$

$$\therefore \quad d_{100} = a = \lambda/2\sin\theta_{100} = 154\text{ pm}/2\sin(7°\ 25') = \mathbf{597\ pm}$$

Similarly, $d_{010} = b = 154\text{ pm}/2\sin 3°\ 28' = \mathbf{1270\ pm}$

$$d_{001} = c = 154\text{ pm}/2\sin 10°13' = \mathbf{434\ pm}$$

Number of molecules in unit cell : The volume of the unit cell,

$$V = abc = 597 \times 1270 \times 434\text{ pm}^3 = 3{\cdot}29 \times 10^{-28}\text{ m}^3$$

$$\therefore \quad \rho = \frac{nM}{VN_A} = \frac{(n)(271{\cdot}5\text{g mol}^{-1})}{(3{\cdot}29 \times 10^{-28}\text{m}^3)(6{\cdot}022 \times 10^{23}\text{ mol}^{-1})}$$

$$= 1{\cdot}37\ n \times 10^6\text{ g m}^{-3} = 1{\cdot}37\ n \times 10^3\text{ kg m}^{-3}$$

$$\rho\text{ (given)} = 5{\cdot}42\text{ g cm}^{-3} = 5420\text{ kg m}^{-3}$$

$$\therefore \quad n = 5420\text{ kg m}^{-3}/1{\cdot}37 \times 10^3\text{ kg m}^{-3} = \mathbf{3{\cdot}97 \approx 4}$$

Since n=4, hence there are **4 molecules of $HgCl_2$ per unit cell.**

Example 16. Calculate the angle at which (*a*) first order reflection and (*b*) second order reflection will occur in an X-ray spectrometer when X-rays of wave length 1·54 Å are diffracted by the atoms of a crystal, given that the interplanar distance is 4·04 Å.

Solution : (*a*) For first order reflection (n=1), the Bragg equation is $2d \sin\theta = \lambda$

$$\therefore \quad \theta = \sin^{-1}(\lambda/2d) = \sin^{-1}(1{\cdot}54\text{ Å}/8{\cdot}08\text{ Å}) = \sin^{-1}(0{\cdot}191) = \mathbf{10°\ 59'}$$

(*b*) For second order reflection (n = 2), the Bragg equation is $2d \sin\theta = 2\lambda$

$$\therefore \quad \theta = \sin^{-1}(\lambda/d) = \sin^{-1}(1{\cdot}54/4{\cdot}04) = \sin^{-1}(0{\cdot}381) = \mathbf{22°\ 24'}$$

Example 17. The density of LiF is 2·601 g cm^{-3}. The (111) first order reflection in the X-ray diffraction from LiF occurs at 8°44′ when X-rays of wave length 70·8 pm are used. If there are four LiF molecules per unit cell, calculate Avogadro's number. LiF crystallizes in the cubic system. Li=6·939, F=18·998.

Solution : $2d_{hkl} \sin\theta_{hkl} = n\lambda$; n=1 for first order reflection

$$\therefore \quad d_{111} = \frac{\lambda}{2\sin\theta_{111}} = \frac{70{\cdot}8\text{ pm}}{2\sin(8°44')} = 233\text{ pm}$$

Also, for the cubic system,

$$d_{hkl} = a/[h^2 + k^2 + l^2]^{1/2}$$

$$\therefore \quad d_{111} = a/[1^2 + 1^2 + 1^2]^{1/2} = a/\sqrt{3} \quad \text{so that } a = \sqrt{3}\ d_{111}$$

Thus, $a = \sqrt{3} \times 233\text{ pm} = 40{\cdot}356\text{ pm} = 403{\cdot}56 \times 10^{-12}\text{ m}$

Density, $\rho = M/V = 2{\cdot}601\text{ g cm}^{-3}\text{ (given)} = 2{,}601\text{ kg m}^{-3}$

Since there are four LiF molecules in the unit cell, hence,

$$M = 4\ (25{\cdot}937\text{ g mol}^{-1}) = 103{\cdot}748\text{ g mol}^{-1} = 103{\cdot}748 \times 10^{-3}\text{ kg mol}^{-1}$$

$$V = N_A a^3 = M/\rho$$

$$\therefore \quad N_A = \frac{M}{\rho\, a^3} = \frac{103{\cdot}748 \times 10^{-3}\text{ kg mol}^{-1}}{(2{,}601\text{ kg m}^{-3})(403{\cdot}56 \times 10^{-12}\text{m})^3} = \mathbf{6{\cdot}49 \times 10^{23}\ mol^{-1}}$$

This value compares very well with the accepted value of $6{\cdot}022 \times 10^{23}$ mol^{-1}.

X-Ray Diffraction Patterns of a Cubic System

It is of particular importance to discuss the X-ray diffraction patterns of a cubic system. We know that for a cubic system, the interplanar distance d_{hkl} is given by

$$d_{hkl} = a/(h^2 + k^2 + l^2)^{1/2} \qquad ...(19)$$

Combining this result with the Bragg equation, *viz.*, $\lambda = 2d_{hkl} \sin \theta_{hkl}$, we get

$$\lambda = \frac{2a \sin \theta_{hkl}}{(h^2 + k^2 + l^2)^{1/2}} \qquad ...(20)$$

$$\therefore \quad \sin^2 \theta_{hkl} = (\lambda^2/4a^2)\,(h^2 + k^2 + l^2) = K(h^2 + k^2 + l^2) \qquad ...(21)$$

where $K = \lambda^2/4a^2$. K has a constant value for a given cubic crystal and a given wave length λ.

We can use Eq. 21 for predicting the diffraction patterns of the three types of lattices of the cubic system, as illustrated below.

1. Primitive Cubic Lattice. Using Eqs. 19 and 21 and integral values (0, 1, 2,...) for the Miller indices *h*, *k*, and *l*, we construct Table 3. It may be noted that since the integer 7 cannot be written in the form $h^2+k^2+l^2$, hence, $\sin^2 \theta$ cannot be equal to $7K$. The diffraction lines will be observed at angles shown in Table 3. The diffraction pattern for a primitive cubic lattice will thus consist of a set of equally spaced six lines followed by an extinction (*i.e.*, a gap) and then another series of six lines.

TABLE 3

Interplanar distances and angles ($\sin^2 \theta_{hkl}$ values) for which diffraction lines are observed for a primitive cubic lattice

hkl	100	110	111	200	210	211	220	300 221	310	311	222	320
d_{hkl}	a	$\frac{a}{\sqrt{2}}$	$\frac{a}{\sqrt{3}}$	$\frac{a}{\sqrt{4}}$	$\frac{a}{\sqrt{5}}$	$\frac{a}{\sqrt{6}}$	$\frac{a}{\sqrt{8}}$	$\frac{a}{\sqrt{9}}$	$\frac{a}{\sqrt{10}}$	$\frac{a}{\sqrt{11}}$	$\frac{a}{\sqrt{12}}$	$\frac{a}{\sqrt{13}}$
$\sin^2 \theta_{hkl}$	K	$2K$	$3K$	$4K$	$5K$	$6K$	$8K$	$9K$	$10K$	$11K$	$12K$	$13K$

2. Body-Centered Cubic Lattice. Using Eqs. 19 and 20 and integral values (0, 1, 2,....) for *h*, *k* and *l*, we construct Table 4. We see that all diffraction lines for which $(h+k+l)$ is an odd integer, are absent. We observe lines at angles shown in Table 4.

TABLE 4

Interplanar distances and angles ($\sin^2 \theta_{hkl}$ values) for which diffraction lines are observed for a body-centred cubic lattice

hkl	100	110	111	200	210	211	220	300 221	310	311	222	320
d_{hkl}		$\frac{a}{\sqrt{2}}$		$\frac{a}{\sqrt{4}}$		$\frac{a}{\sqrt{6}}$	$\frac{a}{\sqrt{8}}$		$\frac{a}{\sqrt{10}}$		$\frac{a}{\sqrt{12}}$	
$\sin^2 \theta_{hkl}$		$2K$		$4K$		$6K$	$8K$		$10K$		$12K$	

3. Face-Centred Cubic Lattice. Proceeding as above, we construct Table 5. We see that the diffraction lines are observed only from those planes for which the values of *h*, *k* and *l* are either all odd or all even. We observe diffraction lines at angles shown in Table 5.

TABLE 5

Interplanar distances and angles ($\sin^2 \theta_{hkl}$ values) for which diffraction lines are observed for a face-centred cubic lattice

hkl	100	110	111	200	210	211	220	300 221	310	311	222
d_{hkl}			$\frac{a}{\sqrt{3}}$	$\frac{a}{\sqrt{4}}$			$\frac{a}{\sqrt{8}}$			$\frac{a}{\sqrt{11}}$	$\frac{a}{\sqrt{12}}$
$\sin^2 \theta_{hkl}$			$3K$	$4K$			$8K$			$11K$	$12K$

The X-ray diffraction patterns for the three types of cubic lattices are collectively shown in Fig. 13.

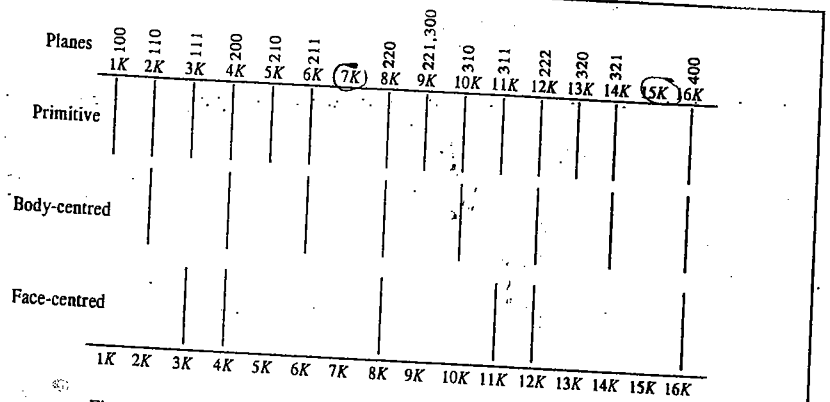

Fig. 13. X-ray diffraction patterns for the three types of cubic lattices.

From the above discussion we see that extinctions (*i.e.*, missing reflections) in the diffraction patterns can help in distinguishing between the three types of cubic lattices. In the X-ray diffraction studies, the crystallographer searches for the missing reflections. It should be noted that whereas the spacing between the lines of a primitive cubic system is equal to K (with a gap after the 6th, 14th and 22nd, etc., lines) the spacing between lines of a body-centred cubic system is equal to $2K$. Thus, the number of lines obtained in the diffraction pattern can help in distinguishing between these two systems. After the identification of the diffraction pattern, it is possible to assign each line with the correct values of the Miller indices *h*, *k* and *l*. From the measurement of any one of these lines, we can determine the value of *a*, the length of the edge of the cube, by using the equation

$$a = (\lambda/2 \sin \theta_{hkl})\,(h^2 + k^2 + l^2)^{1/2} \qquad ...(22)$$

If the lines are indexed correctly, the same value of *a* is obtained from all the values of $\sin \theta_{hkl}$.

X-ray Diffraction Pattern for Tungsten Crystal. The X-ray diffraction pattern for tungsten crystal is shown in Fig. 14.

We notice that there is variation in intensity of the diffracted X-ray beam for different sets of *hkl* planes. This is presumably due to the variation of density of atoms in these planes. The planes having high atomic density give rise to a better X-ray diffraction thereby producing a more intense diffracted beam.

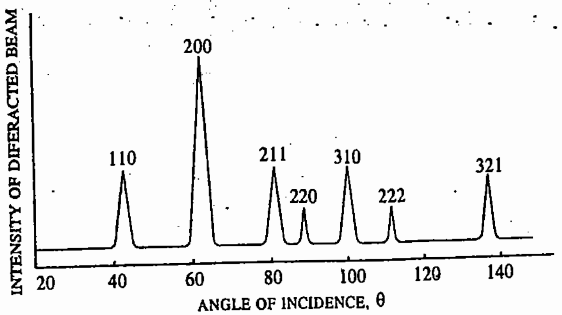

Fig. 14. X-ray diffraction pattern for tungsten crystal.

If the crystal contains more than one kind of atoms, the atom containing greater number of electrons scatters the X-rays to a greater extent. It is found that the *scattering power of an atom is directly proportional to the number of electrons* in the atom. Thus, when the unit cell of a crystal contains hydrogen atoms and other heavier atoms, the scattering effect of hydrogen atoms is overshadowed by that of the other atoms which contain larger number of electrons. Hence, *the positions of hydrogen atoms in the unit cell of a crystal cannot be determined from the X-ray diffraction pattern.* Their positions can be determined by *neutron diffraction.* We shall discuss this aspect a little later in this chapter.

Example 18. **The X-ray diffraction pattern of silver, known to crystallize in the cubic system, was obtained using X-rays with wave length 154·1 pm. The first six lines occurred at the following angles : 19·08°, 22·17°, 32·26°, 38·74°, 40·82° and 49·00°. *(a)* Determine the type of the cubic system, *(b)* Calculate the length of the edge of the cube, *(c)* Calculate the interplanar distance of the plane (111).**

Solution : *(a)* From Eq. 21, $\sin^2\theta_{hkl} = K(h^2 + k^2 + l^2)$ where $K = \lambda^2/4a^2$,

We construct the following table with $K = 0{\cdot}0356$:

θ	19·08°	22·17°	32·26°	38·74°	40·82°	49·00°
$\sin\theta$	0·3268	0·3773	0·5338	0·6257	0·6536	0·7547
$\sin^2\theta$	0·1067	0·1424	0·2848	0·3915	0·4272	0·5696
	$3K$	$4K$	$8K$	$11K$	$12K$	$16K$

Comparing this pattern with that given in Fig. 13, we see that silver crystallizes in **face-centred cubic system.**

(b) From Eq. 22, $a = \dfrac{\lambda}{2\sin\theta_{hkl}}(h^2 + k^2 + l^2)^{1/2}$

The reflection at 19·08° is due to the (111) plane.

$$\therefore \qquad a = \frac{154{\cdot}1\text{ pm}}{2\times 0{\cdot}3268}(1^2 + 1^2 + 1^2)^{1/2} = \mathbf{408{\cdot}6\ pm}$$

(c) From Eq. 13, $d_{hkl} = a/(h^2 + k^2 + l^2)^{1/2}$

$$d_{111} = 408{\cdot}6\text{ pm}/(1^2 + 1^2 + 1^2)^{1/2} = 408{\cdot}6\text{ pm}/\sqrt{3} = \mathbf{235{\cdot}9\ pm}$$

Example 19. **AgCl has a face-centred cubic unit cell whereas CsCl has a body-centred unit cell. Determine which of the following Miller indices are permitted in the X-ray diffraction pattern of *(a)* AgCl and *(b)* CsCl : 100, 010, 001, 200, 020, 002, 110, 101, 011, 120, 102, 012, 210, 201, 021, 220, 202, 022, 111, 222, 221, 212, 122, 211, 121, 112.**

Solution : *(a)* AgCl has a f.c.c. unit cell. So, the only allowed reflections are those in which all indices are even or all are odd, giving Miller indices 200, 020, 002, 220, 202, 022, 111 and 222. Since $a=b=c$, 200=020=002 and 220=202=022 so that only four peaks will be observed corresponding to 200, 220, 111 and 222.

(b) CsCl has a b.c.c. unit cell. So, the only allowed reflections are those in which $h+k+l=$ even, giving 200=020=002 ; 110=101=011 ; 220=202=022 and 211=121=112.

Fourier Synthesis of Electron Density in a Crystal

Since X-rays are scattered by the electrons in a crystal, the ultimate goal of X-ray crystallography is to determine the electron density $\rho(xyz)$ as a function of the coordinates x, y, z. Since the number of electrons and the size of the atomic orbitals both vary from atom to atom, different atoms have different scattering efficiencies. The *scattering factor f* of an atom is defined as

$$f = 4\pi\int_0^\infty \rho(r)\,\frac{\sin kr}{kr}\,r^2 dr \qquad \text{...(23)}$$

where $\rho(r)$ is the spherically symmetric electron density (number of electrons per unit volume) of the atom and $k = (4\pi/\lambda)\sin\theta$ where λ is the wave length of the X-rays and θ is the scattering angle. Since the wave length of the X-rays used for recording the X-ray diffraction pattern is of the size of an atom, the scattered waves from different regions of an atom interfere constructively. The integral in Eq. 23 takes this interference into account through the factor $(\sin kr)/kr$. Before proceeding further we shall prove an important result that the scattering factor of an atom in the direction $\theta \to 0$ is equal to the number of electrons (N_e) in the atom, *i.e.*,

$$\lim_{\theta\to 0} f = N_e \qquad \text{...(24)}$$

Here $\theta \to 0$ implies that the X-rays pass straight through the atom. If $\theta = 0$, then $k = 0$ and the term $(\sin kr)/kr$ in Eq. 23 is indeterminate. Hence, to evaluate the integrand, we evaluate the $\lim\limits_{kr\to 0}(\sin kr)/kr$.

We know from the result of the power series that

$$\lim_{\theta\to 0}\frac{\sin\theta}{\theta} = \lim_{\theta\to 0}\frac{\theta - \dfrac{\theta^3}{3!} + \dfrac{\theta^5}{5!} - \dots}{\theta} \qquad \text{...(25)}$$

$$\approx 1 - \frac{\theta^3}{3!} + \frac{\theta^4}{4!} - \dots \approx 1 \qquad \text{...(26)}$$

Hence, $\lim\limits_{kr\to 0}(\sin kr)/kr = 1$ so that

$$f = 4\pi\int_0^\infty \rho(r)\,r^2 dr = N_e \qquad \text{...(27)}$$

since the integrand is the product of the electron density and the spherical volume element $4\pi r^2 dr$, which upon integration yields the total number of electrons in the atom.

Let us now return to the electron density $\rho(xyz)$ which is so defined that $\rho(xyz)dxdydz$ is the number of electrons in the volume element $dxdydz$. Since the electron density is a periodic function, it can be expanded by a Fourier series :

$$\rho(xyz) = \frac{1}{V}\sum_{h=-\infty}^{\infty}\ \sum_{k=-\infty}^{\infty}\ \sum_{l=-\infty}^{\infty} F(hkl)\exp\left[-2\pi i\left(\frac{hx}{a} + \frac{ky}{b} + \frac{lz}{c}\right)\right] \qquad \text{...(28)}$$

where V is the volume of the unit cell ; x, y, z are the coordinates of a point in the unit cell ; a, b, c are the unit cell dimensions ; (hkl) are the Miller indices and $F(hkl)$ are the Fourier coefficients which are also referred to as the **structure factors.** Each structure factor is associated with a particular reflection from the (hkl) planes. Though the triple summation in Eq. 28 is over all the values ($-\infty$ to $+\infty$) of h, k, l, in practice all the terms need not be included in the summation although the more the terms included, the higher is the resolution of $\rho(xyz)$. The structure factors contain all the information about all the atoms in a unit cell. The structure factor $F(hkl)$ is defined as

$$F(hkl) = \sum_j f_j \exp\left[2\pi i\left(\frac{hx_j}{a} + \frac{ky_j}{b} + \frac{lz_j}{c}\right)\right] \qquad ...(29)$$

where f_j is the scattering factor of the jth atom in the unit cell and the summation is over all the atoms in the unit cell. To account for the above expression for $F(hkl)$, we recall that when the Bragg law is satisfied for a given reflection, the amplitude of the wavelet scattered from an atom in one unit cell of the crystal is in phase with the amplitudes of the scattered wavelets from the corresponding atoms in the millions of the other unit cells of the crystal. However, the wavelet scatterred by one atom may, in general, not be in phase with the wavelet scattered by another atom within the same unit cell with the result that the intensity $I(hkl)$ of reflection will depend upon the extent to which amplitudes of the wavelets reflected from different atoms (denoted by f_j) are in phase with one another. It is known that

$$I(hkl) \propto |F(hkl)|^2 \qquad ...(30)$$

i.e., the intensities of the X-ray diffraction patterns from the (hkl) planes of the crystal are proportional to the square of the modulus (absolute value) of $F(hkl)$. $I(hkl)$ can be determined from the densities of spots on the photographic film. From the values of $I(hkl)$, $|F(hkl)|^2$ can be determined. But the crystallographer needs $F(hkl)$ rather than $|F(hkl)|^2$ to calculate $\rho(xyz)$ with the help of Eq. 28. Since $F(hkl)$ is a complex number, we can write

$$F(hkl) = A(hkl) + iB(hkl) \qquad ...(31)$$

Hence,

$$|F(hkl)|^2 = [A(hkl) + iB(hkl)]\,[A(hkl) - iB(hkl)]$$

$$= [A(hkl)]^2 - [B(hkl)]^2 \qquad ...(32)$$

Since the values of $A(hkl)$ and $B(hkl)$ are not obtained directly, indirect methods are employed to determine these quantities for the evaluation of $F(hkl)$. For a centrosymmetric crystal, $F(hkl)$ is of the form

$$F(hkl) = \pm\, f_{\text{heavy}} \pm f_{\text{light}} \qquad ...(33)$$

where f_{heavy} are the scattering factors of the heavy atoms and f_{light} are the scattering factors of the light atoms. The f_{light} are much smaller than f_{heavy} and their phases are almost random if the atoms are distributed throughout the unit cell. Thus, the heavy atoms dominate scattering since their scattering factors are of the order of their atomic numbers. Since the net result of f_{light} changes $F(hkl)$ only slightly, it follows that $F(hkl)$ will have the same sign as that calculated from the location of the heavy atoms. This phase is then combined with the observed $|F(hkl)|$ obtained from the observed value of $I(hkl)$ to perform the Fourier synthesis of the entire electron density in the unit cell thereby enabling the location of both the heavy and the light atoms. This is how the **phase problem** in crystallography is solved.

Patterson Synthesis. This technique is employed for determining relative orientations of pairs of atoms in a given crystal structure. The technique makes use of the Patterson equation, *viz.*,

$$P(\vec{r}) = \frac{1}{V}\sum_{h=-\infty}^{\infty}\sum_{k=-\infty}^{\infty}\sum_{l=-\infty}^{\infty}|F(hkl)|^2 \exp\left[-2\pi i\left(\frac{hx}{a} + \frac{ky}{b} + \frac{lz}{c}\right)\right] \qquad ...(34)$$

The values of $|F(hkl)|^2$ can be obtained without ambiguity from the value of $I(hkl)$. The Patterson equation is manifested in the form of a map of *vector separation* between the atoms in the unit cell. Thus, if (x_A, y_A, z_A) and (x_B, y_B, z_B) are, respectively, the coordinates of atoms A and B in the unit cell, then there would occur a peak at $(x_A-x_B, y_A-y_B, z_A-z_B)$ and also at $(x_B-x_A, y_B-y_A, z_B-z_A)$ since there is a vector from B to A as well as a vector from A to B. The height of the peak in the map is proportional to the product Z_AZ_B where Z_is are the atomic numbers. Thus, the relative orientation of each pair of atoms in the original structure can be obtained from the Patterson map. This technique was used extensively by the British crystallographer Dorothy Hodgkin (1910–1994) during 1940–1960 to determine the structures of important biochemical substances. She was awarded the 1964 Chemistry Nobel Prize for her work.

More advanced techniques, known as direct methods, were developed in the 1950s by the American crystallographers H. Hauptman and J. Karle for the determination of crystal structures. The discussion of these methods is, however, beyond the scope of the present volume. Hauptman and Karle were awarded the 1985 Chemistry Nobel Prize for their contributions.

Example 20. Calculate the structure factor $F(hkl)$ values for the three types of cubic lattices, *viz.*, the primitive cubic (P), body centred cubic (I) and face-centred cubic (F) and therefrom determine which reflections would be absent from the diffraction pattern. The fractional coordinates (x_j, y_j, z_j) of the atoms in the three types of lattices are :

P : (0, 0, 0) ; I : (0, 0, 0) and (1/2, 1/2, 1/2) and F : (0, 0, 0), (1/2, 1/2, 0), (1/2, 0, 1/2) and (0, 1/2, 1/2)

Solution : This example illustrates the use of the structure factors to distinguish between the three types of cubic lattices.

For the primitive cubic (P) lattice,

$$F(h\,k\,l) = \sum_j f_j \exp\left[2\pi i\left(\frac{hx_j}{a} + \frac{ky_j}{b} + \frac{lz_j}{c}\right)\right]$$

$$= \sum_j f_j \qquad \text{(since } x_j, y_j, z_j \text{ are zero and } e^0=1\text{)}$$

Thus, $F(hkl)$ has the same value for all h, k and l. Hence there would be reflections in the diffraction pattern for all integral values of h, k and l.

For the body-centred cubic (I) lattice,

$$F(h, k, l) = f\exp[2\pi i(0 + 0 + 0)] + f\exp[2\pi i(h/2 + k/2 + l/2)]$$

$$= f\left[1 + \exp i\pi(h+k+l)\right]$$

Recalling that $e^{i\theta} = \cos\theta + i\sin\theta$ (Euler's relation) with $\theta=\pi$, we have

$$e^{i\pi} = \cos\pi + i\sin\pi = -1$$

Thus, $F(h, k, l) = f\,[1 + (-1)^{h+k+l}]$

If $(h+k+l)$ is even, $F(h,k,l) = 2f$ and if $(h+k+l)$ is odd, $F(hkl) = 0$. Thus, in the X-ray diffraction pattern, reflections such as (110), (200), (211), (310), etc., will be present and reflections such as (100), (111), (210), (300), etc., will be absent.

For the face-centred cubic (F) lattice,

$$F(hkl) = f\exp[2\pi i(0+0+0)] + f\exp[2\pi i(h/2+k/2+0)] + f\exp[2\pi i(h/2+0+h/2)] + f\exp[2\pi i(0 + k/2 + l/2)]$$

$$= f\,[1 + \exp(i\pi(h+k)) + \exp(i\pi(h+l) + \exp(i\pi(k+l)]$$

$$= f\,[1 + (-1)^{h+k} + (-1)^{h+l} + (-1)^{k+l}]$$

If h, k, l are all even or all odd, $F(hkl) = 4f$ and these reflections will be present. If one is even and the other two are odd, or the reverse, then these reflections will be absent.

ELECTRON DIFFRACTION

The wave-particle duality of matter was proposed by the French physicist Louis de Broglie in 1924. According to de Broglie's hypothesis, the wave length λ of electrons moving with velocity v is given by $\lambda = h/(m_eV)$, where m_e is the mass of the electron. Electrons can be accelerated to precisely controlled energies by applying a known potential difference. When accelerated through 10 keV, they acquire a wave length of 12 pm which makes them suitable for molecular diffraction investigations. Electron diffraction studies generally utilize electrons with energies of the order of 40 keV. Since electrons are charged, they are scattered strongly by their interaction with electrons and nuclei of atoms of the sample. Hence, they cannot be used for studying the interiors of solid samples. They can, however, be used for studying molecules in the gaseous state held on surfaces and in thin films. The most important application involves the study of electron diffraction by substances in their vapour state at low pressures (of the order of 10^{-5} torr). The strong interaction of electrons with molecules of the sample plus a very great effect on the photographic plate combine to require a very short exposure of the order of tenths of a second.

Whereas the diffraction of X-rays by a crystal depends upon the spacing between the layers, *the diffraction of electrons by gaseous molecules depends upon the distances between the atoms in a molecule.* Since the gaseous molecules are randomly oriented relative to the electron beam, the diffraction pattern, like that of an X-ray powder photograph, consists of concentric rings. There is an appreciable amount of background scatter of the electron beam with the result that diffraction bands are only poorly resolved. New experimental techniques have, however, greatly improved the resolution of the bands.

It is possible to calculate the electron scattering from a pair of nuclei separated by a distance R_{ij} and oriented at a definite angle to the incident beam. The overall diffraction pattern is then calculated by allowing for all possible orientations of this pair of atoms. This procedure amounts to integration over all possible orientations. The final expression obtained for the diffraction intensity is

$$I_{ij}(\theta) = 2f_if_j\,\{(1 + \sin sR_{ij})/sR_{ij}\} \qquad \text{...(35)}$$

where $s = -(4\pi/\lambda)\sin(\theta/2)$, λ is the wave length of electron beam and θ is the scattering angle. The quantities f_i and f_j are the scattering factors of the ith and jth atoms. They determine the scattering power of the atoms. If a molecule consists of a number of atoms, the total intensity is given by the **Wierl equation,** *viz.*,

$$I(s) \propto \sum_{i,j} f_if_j \frac{\sin sR_{ij}}{sR_{ij}} \qquad \text{...(36)}$$

where the summation is over all the atoms i and j of the molecule. The electron diffraction pattern can be interpreted in terms of the distances between all possible pairs of atoms in the molecule (not simply those bonded together). The Wierl equation does not, unfortunately, allow the direct calculation of the internuclear distances R_{ij} from the measurements of $I(s)$ at various values of s.

The electron diffraction studies are useful for evaluating the bond lengths and bond angles in relatively simple gaseous molecules. As the number of atoms in the molecules increases, one soon reaches the situation where the number of pieces of information available (*viz.*, the spacings of the resolved diffraction rings) is not great enough to evaluate all of the necessary structural parameters. The number of electron diffraction rings observed is usually much less than the number of X-ray diffraction spots observed in the X-ray crystal study. This shows that difficulties lie in the path of structure determination by electron diffraction. In spite of these difficulties, however, many molecular structures have been determined by this method. The accuracy of bond length and bond angles obtained from electron diffraction studies is comparable to that obtained from X-ray diffraction studies for simple molecules.

NEUTRON DIFFRACTION

As dissussed above, diffraction patterns can be obtained by means of electron beams when they are scattered by molecules. Because of their negative charge and hence low penetrating power, the electron beams are generally used for the investigation of surfaces and thin films. Neutrons, on the other hand, have a high penetrating power and are particularly useful for structural studies of solids. Neutron diffraction by crystals was demonstrated as early as in 1936 but the method did not become important until the advent of nuclear piles. Fast neutrons produced in a nuclear pile are slowed down by collisions with a moderator (D_2O or graphite) to produce thermal neutrons, *i.e.*, neutrons for which the range of kinetic energies is determined by the temperature of the surroundings.

The wave length of a neutron beam is related to the neutron mass and velocity by de Broglie relation $\lambda = h/p = h/m_nv$, where m_n is the neutron mass and v its velocity. The spectrum of the neutron beam emerging from a nuclear pile is continuous, the wave lengths covering several Angstroms. A monochromatic beam which is used for neutron crystallography, is obtained by reflection at a flat crystal surface. Wide beams, with cross-sectional areas of a few square centimetres, are used in order to obtain a sufficiently high counting rate in the detector. The large size and high cost of neutron spectrometers combined with the need for a nuclear pile have made neutron diffraction a less popular method in crystallography.

Whereas X-rays are scattered by the orbital electrons, the neutrons are scattered by atomic nuclei. The atomic nuclei contribute nothing to X-ray scattering. Neutron diffraction is caused by two additional factors : (1) *nuclear scattering* due to the interaction of neutrons with the atomic nuclei and (2) *magnetic scattering* due to the interaction of the magnetic moments of neutrons with permanent magnetic moments of atoms or ions. The X-ray scattering power increases fairly regularly with the atomic number but there is no regular trend for neutron scattering. The neutron scattering power does not vary greatly while the X-ray scattering power increases from hydrogen atom to the heavy elements by about three orders of magnitude. In uranium hydride, X-ray diffraction has been used to locate the uranium coordinates and neutron diffraction to locate the hydrogen coordinates.

The differences between neutron and X-ray scattering offer great advantages and equally great disadvantages to neutron crystallography. The major advantage is that light elements such as H or D, which cannot be located by X-ray diffraction, can be located by neutron diffraction because they are comparable in neutron scattering power to heavy elements. The great disadvantage is that the background scatter is likely to be much more serious because different isotopes of the same element, which would be expected to be randomly distributed among the sites for that element, might differ greatly in their scattering power.

Neutrons which possess magnetic moment by virtue of having a spin of 1/2, interact with nuclei which have magnetic moments to produce further background scattering for substances for which the nuclear spins are randomly oriented. The spin-disorder scattering is so great for hydrogen in comparison with the ordered scattering that deuterated compounds are often used for neutron diffraction studies. Paramagnetic substances also contribute to the general background scattering because of the interaction of the magnetic moments of neutrons with the randomly oriented orbital magnetic moments of the electrons. The magnetic moments of neighbouring atoms are oriented in the *same direction in ferromagnetic substances* whereas the magnetic moments of neighbouring atoms are oriented *in opposite directions in antiferromagnetic substances*. Neutron diffraction thus offers a tool for the investigation of the magnetically ordered lattices. Neutron diffraction is reserved for special applications for which it can yield information not obtainable from X-ray diffraction studies. The Canadian physicist B.N. Brockhouse and the American physicist C.G. Shull were awarded the 1994 Physics Nobel Prize for the development of neutron spectroscopy and neutron diffraction techniques.

TYPES OF CRYSTALS

It is convenient to classify solid crystals into the following four types :

1. Molecular crystals in which the units occupying the lattice points are molecules.
2. Covalent crystals in which the units are atoms.
3. Ionic crystals in which the units are positively and negatively charged ions.
4. Metallic crystals in which the units are positive metallic ions surrounded by a 'sea' of electrons.

The main characteristics of the various types of crystals are summed up in Table 6.

TABLE 6

Characteristics of Various Types of Crystals

Characteristics	Molecular crystals	Covalent crystals	Ionic crystals	Metallic crystals
Units that occupy lattice points	Molecules	Atoms	Positive and negative ions	Positive ions in a 'sea' of electrons
Binding force	*(i)* van der Waals *(ii)* Dipole-dipole	Shared electrons	Electrostatic attraction	Electrical attraction between +ive ions and – ive electrons
Physical properties	Very soft Low melting points Good insulators	Very hard Very high melting points Non-conductors	Quite hard and brittle Fairly high melting points Semi-conductors due to crystal imperfections	Hard or soft Moderate to high melting points Good conductors
Examples	NH_3, H_2O, CO_2	Diamond, carborundum, quartz	NaCl, KNO_3 Na_2SO_4	Na, Cu, Fe

Some further description of these crystals is given below.

Molecular Crystals

The lattice points in molecular crystals consist of specific molecules which do not carry any charge. The forces binding the molecules together are of two types : *(i) Dipole–dipole forces (ii) The van der Waals forces.* Dipole–dipole forces occur in solids which consist of polar molecules. Thus, in the case of water molecules (in ice or even in liquid state), the negative end of one molecule attracts the positive end of a neighbouring molecule, as shown in Fig. 15.

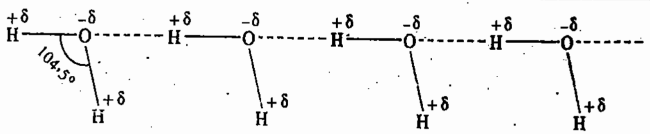

Fig. 15. Dipole–dipole forces of attraction between water molecules.

The van der Waals forces are more general and occur in all kinds of molecular crystals. Both types of molecular forces mentioned above are much weaker than the coulombic forces of attraction between oppositely charged ions existing in ionic crystals. The binding energy in molecular crystals, therefore, is considerably less than in ionic crystals. Accordingly, the heat of vaporisation, *i.e.*, the energy required to separate molecules from one another in a molecular crystal is very low in comparison to the value for ionic or covalent crystals. The molecular crystals are, therefore, more volatile and have lower melting and boiling points.

On account of weak forces binding the molecules together, molecular crystals are usually soft, easily compressible and can be easily distorted. Since no ions or charged particles are present, molecular crystals are bad conductors of electricity in solid, liquid as well as in dissolved state.

Covalent Crystals

The lattice in covalent crystals consists of atoms linked together by a continuous system of covalent bonds. Diamond furnishes a good example of this type. Its structure is represented in Fig. 16.

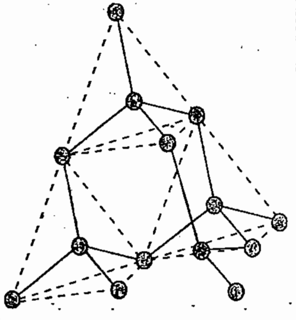

Fig. 16. Structure of diamond.

Each carbon atom is covalently bonded by sharing of electrons to four other atoms involving sp^3 hybrid orbitals. Thus each carbon atom is surrounded by four others at the four corners of a regular tetrahedron. This gives rise to a rigid three-dimensional network. This is the reason why diamond is the hardest substance known, with a high density and melting point. The entire crystal is regarded as one large carbon molecule and is called a *macromolecule.*

In some crystals belonging to this type, the continuous network of covalent bonds is two-dimensional. Graphite offers a very good example. Its structure is represented in Fig. 17. Each carbon atom is covalently bonded to three others involving sp^2 hybrid orbitals instead of four as in diamond. Thus, all atoms in a single plane are linked to give flat hexagons as in benzene, naphthalene, anthracene, etc. The hexagons are held together in sheet-like structures, parallel to one another. The C—C covalent bond distance is 1·42 Å. The distance between the sheets or layers, however, is comparatively large being about 3·35 Å. This rules out the possibility of covalent bonding between the layers. Such crystals in which the various sheets of atoms are separated from one another by a distance larger than the maximum permissible for the formation of chemical bond are said to have layer lattices.

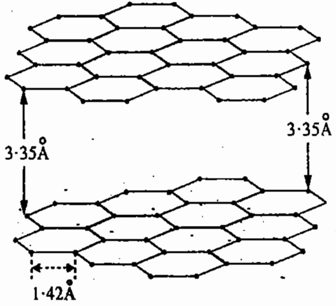

Fig. 17. Structure of graphite.

Since a chemical bond is not possible between carbon atoms in different layers, the fourth valency remains unsatisfied, *i.e.*, some electrons remain free or unpaired. This permits the passage of electricity through graphite making it a good conductor of electricity.

As the cohesive forces between different layers or sheets are relatively feeble, rupture between the various layers can occur easily. Such substances, therefore, are soft. They are used as lubricants because one plane of atoms can readily slip over another.

Ionic Crystals

In ionic crystals, the units occupying lattice points are positive and negative ions. In sodium chloride, for example, the units are Na^+ ions and Cl^- ions. Each ion of a given sign in held by coulombic forces of attraction to all ions of opposite sign. These forces are very strong and, therefore, the amount of energy required to separate ions from one another is very high. Accordingly, the ionic crystals have the following characteristics :

1. The heats of vaporisation of ionic crystals are high.
2. The vapour pressures of ionic crystals at ordinary temperatures are very low.
3. The melting and boiling points of ionic crystals are very high.
4. Ionic crystals are hard and brittle.
5. Ionic crystals are insulators in the solid state. The reason is that ions are entrapped in fixed places in the crystal lattice and cannot move when electric field is applied. However, when melted, they become good conductors of electricity. This is due to the fact that in the molten state, the well-ordered arrangement of ions in the crystals is destroyed and the ions are in a position to move about in the liquid medium when an electric field is applied.
6. Ionic crystals are soluble in water and also in other polar solvents. They are insoluble or very slightly soluble in non-polar solvents such as benzene and carbon tetrachloride.
7. Ionic solids are good conductors when dissolved in water. The ions held by coulombic forces fall away from one another when dissolved in water or in any other solvent having high dielectric constant. This is in accordance with the Coulomb's law that forces of attraction between oppositely charged particles vary inversely as the dielectric constant.

Characteristic Structures of Ionic Crystals. The ionic model treats a crystal as an assembly of oppositely charged spheres that interact primarily through coulombic forces. If the thermo-dynamic properties of the crystal calculated on the basis of the ionic model agree with experiment, the crystal may be taken as ionic. We shall briefly discuss the characteristic structures which are prototypes of a wide range of ionic crystals

1. The Rock Salt (NaCl) Structure. This structure is based on an f.c.c. array of bulky anions in which the cations occupy all the octahedral holes (Fig. 18). Alternatively, it can also be treated as a structure in which anions occupy all the octahedral holes in an f.c.c. array of cations. It is evident from the diagram that each ion is surrounded by an octahedron of six counter ions. Thus, the coordination number (C.N.) of each type of ion is 6 and the structure is referred to as (6 : 6) coordination. In this notation, the first number in the parenthesis is the coordination number of the cation and the second number is the coordination number of the anion.

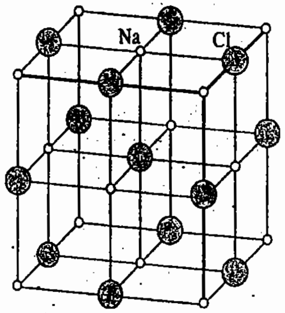

Fig. 18. The rock salt structure.

In order to determine the number of ions of each type in a unit cell, the following rules should be borne in mind :

(*i*) An ion in the body of a unit cell belongs entirely to that unit cell and counts as 1.

(*ii*) An ion in a face is shared by two unit cells and contributes 1/2 to the unit cell in question.

(*iii*) An ion on an edge is shared by four unit cells and thus contributes 1/4.

(*iv*) An ion at a vertex is shared by eight unit cells that share the vertex and so contributes 1/8.

Applying the above rules to the rock salt (NaCl) structure, we find that there are four Na^+ ions and four Cl^- ion so that each unit cell contains four NaCl formula units.

The structure of KCl crystal is similar to that of NaCl crystal.

2. The Cesium Chloride Structure. This structure (Fig. 19) has a cubic unit cell with each vertex occupied by an anion having a cation at the centre of the unit cell (or vice versa). The coordination number for both types of ions is 8 and the structure is referred to as (8 : 8) coordination.

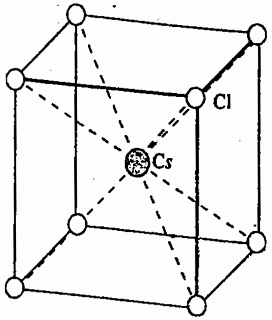

Fig. 19. The cesium chloride structure.

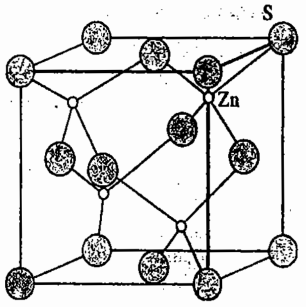

Fig. 20. The sphalerite (zinc blende) structure.

3. The Zinc Blende (Sphalerite) Structure. This structure (Fig. 20), deriving its name from the mineral form of ZnS, is based on an expanded f.c.c. anionic lattice where cations occupy one type of tetrahedral holes. Each anion is surrounded by four neighbours. Thus the structure has (4 : 4) coordination.

4. The Wurtzite Structure. This structure (Fig. 21) differs from the zinc blende structure in being derived from an expanded hexagonally close packed array of anions rather than an f.c.c. array. However, as in the zinc blende structure, the cations occupy one type of tetrahedral holes. The structure, thus, has a (4 : 4) coordination.

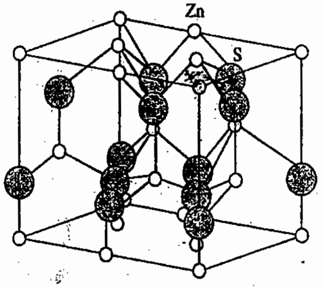

Fig. 21. The wurtzite structure.

5. The Fluorite Structure. This structure (Fig. 22) takes its name from CaF_2. In this structure, the cations occupy half the cubic holes of a primitive cubic array of anions. Alternatively, the anions occupy both types of tetrahedral holes in an expanded f.c.c. lattice of cations. (In the **antifluorite structure**, an example of which is K_2O, the roles of the cations and anions are reversed). In the fluorite structure, the coordination number is 8 for the cations (eight fluoride ions forming a cube about each calcium ion) and 4 for the anions (four Ca^{2+} ions tetrahedrally arranged about each F^- ion). Thus, the fluorite structure has (8 : 4) coordination.

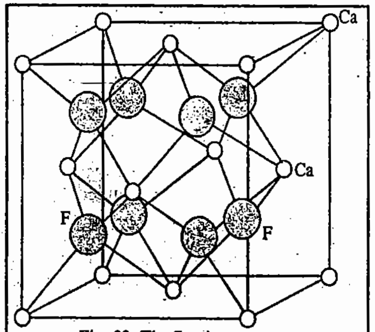

Fig. 22. The fluorite structure.

6. The Rutile Structure. This structure (Fig. 23) takes its name from **rutile**, the mineral form of titanium (IV) oxide, TiO_2. The coordination numbers are 6 for the cations (six oxide anions arranged approximately octahedrally about the Ti^{4+} ions) and 3 for the anion (three Ti^{4+} ions arranged trigonally about the oxide ions). The rutile structure has, thus, (6 : 3) coordination.

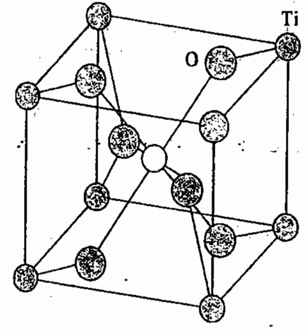

Fig. 23. The rutile structure.

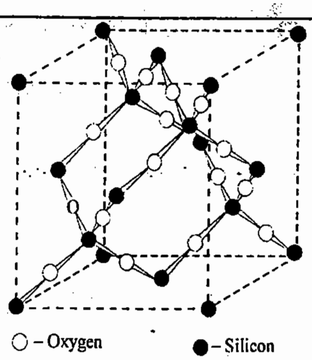

Fig. 24. The β-cristobalite structure.

7. The β-Cristobalite Structure. SiO_2 crystallizes in several forms, one of which is β-cristobalite (Fig. 24) which is related to the zinc blende structure. It has silicon atoms in place of zinc and sulphur atoms with oxygen atoms lying in between the silicon atoms.

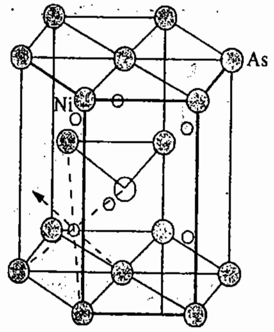

Fig. 25. The nickel arsenide structure.

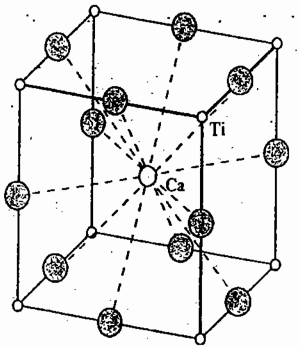

Fig. 26. The perovskite structure.

In addition to the above mentioned seven types of structures of ionic solids, we have three more structures. These are the **nickel arsenide structure** (Fig. 25), the **perovskite structure** (Fig. 26) and the **spinel structure** (Fig. 27). The *nickel arsenide structure* is based on an expanded, distorted *hcp* anionic array with cations occupying the octahedral holes. The *perovskite structure*, the prototype of which is the mineral calcium titanate, $CaTiO_3$, is cubic with Ca atoms surrounded by 12 oxygen atoms and the titanium atoms surrounded by 6 oxygen atoms. The *spinel structure*, typified by $MgAl_2O_4$, consists of an f.c.c. array of O^{2-} ions in which Mg^{2+} cations occupy one-eighth of the tetrahedral holes and Al^{3+} cations occupy the octahedral holes.

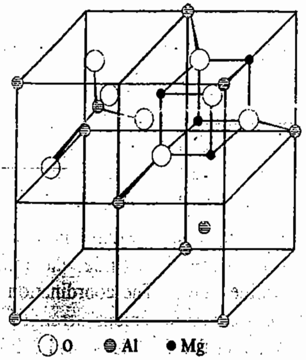

Fig. 27. The spinel structure.

METALLIC CRYSTALS

Metals are characterised by high electrical and thermal conductivity, bright lustre, malleability, ductility and high tenstile strength. It has been observed that metals, generally, have *low* ionisation energies because the valency electrons (*i.e.*, the electrons in the outermost shell) can be taken out relatively easily. This implies that valency electrons in metals are weakly bound to the kernel (by kernel, we mean the nucleus and electrons other than those in the outermost shell).

Consider the case of lithium. It has one valency electron, the electronic configuration being $1s^2$ $2s^1$. The X-ray examination of a crystal of lithium shows that each lithium atom is surrounded by eight other lithium atoms. It is not possible for one lithium atom to get bonded to eight other atoms through covalent bonds, *i.e.*, electron pair bonds, as it contains only one valency electron. But it has other valency orbitals (*viz.*, $2s$, $2p_x$, $2p_y$, $2p_z$) available. Hence, besides its own valency electron, the valency electrons of the neighbouring atoms can also come quite close to its nucleus. In other words, there can be complete freedom of movement of electrons in the vacant valency orbitals around the nucleus of each lithium atom. The valency electrons of metallic atoms, thus, are not localized at each atom. They do not belong to one atom in particular. They are mobile and move about from one kernel to another in the crystal. They are, in effect, a common property of all the atoms present in a metallic crystal.

Electron Sea Model. To account for the nature of bonding in metals, H.A. Lorentz proposed a model known as **'electron sea' model.** According to this model, a metal behaves as if it is an assemblage of positive ions (kernels) immersed in a 'sea' of mobile electrons (Fig. 28). Thus, each electron belongs to a number of positive ions and each positive ion belongs to a number of electrons. The force that binds a metal atom to a number of electrons within its sphere of influence is known as a **metallic bond.**

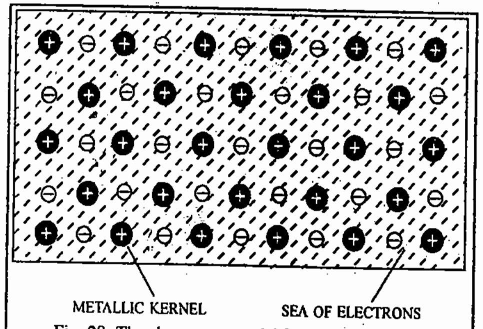

Fig. 28. The electron sea model for metallic atoms.

Explanation of Metallic Properties. All the metallic properties such as electrical and thermal conductivity, bright lustre, malleability, ductility, elasticity, etc., can be explained satisfactorily on the basis of the metallic structure described above.

1. The high electrical conductivity of metals, for example, is due to the presence of the mobile valency electrons. They move readily in an electric field and thus conduct electricity throughout the metal from one end to the other.

2. The high thermal conductivity is also due to the presence of these mobile electrons. If one part of a metal is heated, the electrons in that part acquire a large amount of kinetic energy. Being free, these electrons move rapidly through the crystal and convey heat (*i.e.*, conduct heat) to other parts of the metal.

3. The bright metallic lustre can also be explained as due to the presence of these highly mobile electrons. As a beam of light comprising of electromagnetic waves falls on the surface of a metal, the electric field associated with light waves sets the electrons present on the surface of the metal into to and fro oscillations. Since a moving charge always emits electromagnetic energy, hence, oscillating electrons emit electromagnetic energy in the form of light. Thus, when light falls on a metal surface, it appears as if light is being reflected. The surface, therefore, emits the typical metallic lustre.

4. The model of free valency electrons can also explain the softness, malleability and ductility

associated with metals. The metallic bond holding the positive ions (say, M^+) and the valency electrons is *non-directional*, as already mentioned. In other words, the force of attraction between the M^+ ions and the valency electrons is uniform in all directions. There are no localized bonds. Also the bonds holding the crystal lattice in metals are not rigid as in covalent solids such as ice. The result is that M^+ ions can be easily moved from one lattice site to another. In terms of the crystal, nothing has been changed. The environment of each metal ion remains the same as before since delocalized electrons are available everywhere.

The nearest neighbours can thus be changed easily and new metal bonds can be formed readily. This explains why metals are malleable, *i.e.*, they can be flattened out into thin sheets when hammered. A crystal of ice, on the other hand, is hard. It is neither malleable nor ductile. It is brittle, *i.e.*, it breaks into small pieces when hammered. This is obviously due to the fact that atoms in water molecules (oxygen and hydrogen) are covalently bonded to each other. Covalent bond is rigid and highly directional.

The ease with which the metal ions can be moved from one lattice site to another is also responsible for the fact that the metals are *ductile, i.e.*, they can be drawn into wires by very little expenditure of energy. This also explains why metals like sodium and potassium are soft and can easily be cut with a knife.

5. Metals have high tensile strength, *i.e.*, they can resist stretching without breaking. This is due to the existence of strong electrostatic attraction between the positively charged metal ions and the 'sea' of negative electrons surrounding them. Substances which have covalent bonds, do not possess high tensile strength. This is due to the absence of electrostatic forces of attraction in the crystal, there being no oppositely charged units in the lattice.

6. Metals possess elasticity. Elasticity is a property by virtue of which a substance can resist a deforming force or a property by virtue of which a substance can recover its original form soon after the removal of the deforming force. The elasticity of metals is also due to the ease with which metal ions can move from one lattice site to another.

7. The delocalized electron model can also explain the well known observation that only a small force is needed to bend a straight copper wire sharply. However, straightening out of a bent wire is not so easy. It requires much more force to do so. Not only that ; a small kink always remains. The reason is that the formation of a sharp bend amounts to separation of some of the metal ions from their adjacent electrons and also from their nearest ion neighbours. The previous pattern of ions and electrons is disturbed and a new pattern is set up in the crystal giving rise to new planes and new edges. It is not so easy to restore the previous pattern because the new planes and edges formed during the bending do not ordinarily fit together to restore the original pattern once again.

The electron sea model, however, cannot explain vast variations in properties of certain metals. For example, while mercury melts at such a low temperature as − 39°C, tungsten melts at such a high temperature as 3300°C. While metals, in general, are good conductors of electricity, copper is more than 50 times better conductor than bismuth. Similarly, while metals like sodium and potassium are so soft that they can be cut easily with a knife, osmium is so hard that it can scratch even glass.

Free Electron Model. The free electron model gives a deeper insight into the cause of high electrical conductivity of metals than the electron sea model. In this model each valence electron of the metal is treated as particle in a three-dimensional box of the size of the metal crystal. As discussed in Chapter 1, the energy levels of an electron in an atom are given by the expression

$$E_n = n^2h^2/8m_ea^2 \qquad (n = 1, 2, 3...) \qquad ...(37)$$

where m_e is the mass of the electron and a is the width of the box of infinite height. For each eigenstate, there are two states of the electron corresponding to the two values of the electron spin.

It can be shown that the density of states (DOS) function, $g(\varepsilon)$, is given by

$$g(\varepsilon) = C\varepsilon^{1/2} \qquad ...(38)$$

where C is a constant. The number of one-electron states with energy between ε and $\varepsilon + d\varepsilon$ is given by $g(\varepsilon)d\varepsilon$. The DOS function, $g(\varepsilon)$; is plotted as a function of energy ε in Fig. 19(*a*). As electrons are added at 0 K, the energy levels are filled up to some maximum energy called the Fermi energy, ε_F, determined by the number of electrons. This is indicated by the cross hatching in Fig. 29. The Fermi energy is, in fact, the electrochemical potential of the electrons and determines their tendency to move at an interface. The same information can be obtained by plotting $g(\varepsilon)/\varepsilon^{1/2}$ versus ε as shown in Fig. 29(*b*).

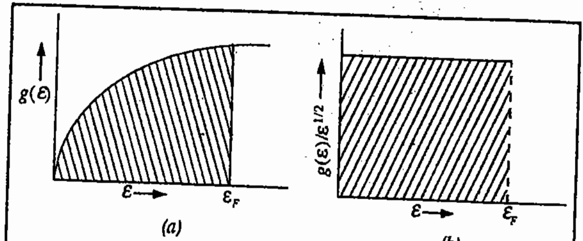

Fig. 29. (*a*) DOS function for a free electron gas as a function of energy (*b*) $g(\varepsilon)/\varepsilon^{1/2}$ versus energy for a free electron gas. The cross-hatching indicates the energy levels occupied at 0 K.

Free electrons having spin equal to $\frac{1}{2}$ obey Fermi-Dirac statistics and are called fermions (Chapter 25). Only one fermion occupies each energy state of the system. At a temperature above 0 K, the number of occupied states with energy range ε to $\varepsilon + d\varepsilon$ is given by

$$d(N/V) = f(\varepsilon, T)g(\varepsilon)d\varepsilon \qquad ...(39)$$

where $f(\varepsilon, T)$ is the Fermi-Dirac distribution function. The function $f(\varepsilon, T)$ is related with ε and T as follows :

$$f(\varepsilon, T) = \frac{1}{\exp[(\varepsilon - \mu)/k_BT)] + 1} \qquad ...(40)$$

where μ is a constant.

When $\varepsilon = \mu$, $f(\varepsilon, T) = 1/2$. Thus, the quantity μ is equal to energy at which $f(\varepsilon, T)$ has half its maximum value. At 0 K, $f(\varepsilon, 0) = 1$ for energies ε less than the Fermi energy, ε_F and $f(\varepsilon, 0) = 0$ for energies ε greater than ε_F. As $T \to 0$, $\mu \to \varepsilon_F$. Thus, it is a good approximation to take $\mu \approx \varepsilon_F$ at any other temperature as well provided $\varepsilon_F >> k_BT$.

Using this approximation and combining Eq. 39 with Eq. 40, we obtain

$$d(N/V) = \frac{C\varepsilon^{1/2}d\varepsilon}{\exp[(\varepsilon - \varepsilon_F/k_BT) + 1} \qquad ...(41)$$

Fig. 30 shows distribution of electron energies at temperatures T_1 and T_2 where $0 < T_1 < T_2$. At room temperature, the distribution of electron energies differs only slightly from that at 0 K for ε_F = 5eV. A small fraction of electrons have energies greater than ε_F ; they leave behind holes in the lattice when they are excited. *The holes and the excited electrons both contribute to electrical conductivity*, σ. This is how the free electron model of metals accounts for high electrical conductivity of metals. It predicts an infinite

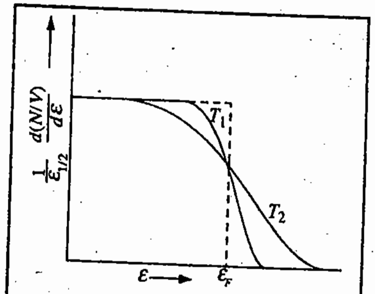

Fig. 30. Distribution of electron energies in a metal at 0 K (dotted line) and two higher temperatures $T_2 > T_1$.

value of σ because the excited electrons can, in principle, be excited to infinite velocities. However, in a metal crystal, the scattering of electrons from the vibrating atoms produces friction which restricts the mobility of the electrons. Electrical conductivity σ is given by

$$\sigma = neu \qquad \text{...(42)}$$

where n is the number of electrons per unit volume, e is the electronic charge and u is the electron mobility.

The free electron model of metals discussed above is only a special case of the more general model, *viz.*, the band model of metals. The Fermi energy is mathematically given by the expression,

$$\varepsilon_F = h^2/8m_e\,(3N/\pi V)^{2/3} \qquad \text{...(43)}$$

where N is the number of valence electrons per mole of the metal and V is the molar volume of the metal. At temperature above 0 K, the electronic kinetic energy per mole is given by

$$\varepsilon = \frac{3}{5}N\varepsilon_F\left[1 + \frac{5\pi^2}{12}\left(\frac{kT}{\varepsilon_F}\right)^2 + \dots\dots\dots\dots\right] \qquad \text{...(44)}$$

The electronic contribution to thermal energy is given by

$$\varepsilon_{thermal} = \varepsilon_r - \varepsilon_0 = \pi^2 N(kT)^2/4\varepsilon_F \qquad \text{...(45)}$$

where ε_r is the internal energy of the metal at some temperature T and ε_0 is the internal energy of the metal at 0 K.

We may mention here that deeper insight into the metallic state has been provided by L. Pauling, N.F. Mott, P.W. Anderson and A.H. Cottrell. The great Indian chemist C.N.R. Rao, who has contributed to several areas of structural chemistry, is another pioneer here. Mott and Anderson have given new theoretical insights on metals. Mott is best known for the metal–insulator transition and A.H. Cottrell is one of the founding fathers of modern metallurgy.

Example 21. Calculate the Fermi energy of sodium metal, given that the density (ρ) of the metal is 0·97 g cm^{-3} and the atomic mass is 23 g mol^{-1}.

Solution : $\rho = 0{\cdot}97 \text{ g cm}^{-3} = 0{\cdot}97\times10^3 \text{ kg m}^{-3}$

The molar volume V of Na metal is given by

$$V = \frac{M}{\rho} = \frac{23\times10^{-3}\,\text{kg mol}^{-1}}{0{\cdot}97\times10^3\,\text{kg m}^{-3}} = 2{\cdot}37\times10^{-5}\ \text{m}^3\ \text{mol}^{-1}$$

Since one atom of Na contains one valence electron, therefore, the number of valence electrons per mole of the metal is $N=6{\cdot}022\times10^{23}$. Thus,

$$\varepsilon_F = \frac{h^2}{8m_e}\left(\frac{3N}{\pi V}\right)^{2/3} \qquad \text{(Eq. 43)}$$

$$= \frac{(6{\cdot}626\times10^{-34}\,\text{J s})^2}{8(9{\cdot}107\times10^{-31}\,\text{kg})}\left[\frac{3(6{\cdot}022\times10^{23}\,\text{mol}^{-1})}{\pi(2{\cdot}37\times10^{-5}\text{m}^3\,\text{mol}^{-1})}\right]^{\frac{2}{3}} = \mathbf{5{\cdot}04\times10^{19}\ J} \quad (\text{J} = \text{kg m}^2\ \text{s}^{-2})$$

Example 22. Calculate the electronic contribution to the thermal energy at 25°C in sodium metal, given that the Fermi energy of Na is 5·04×10^{-19} J.

Solution :

$$E_{thermal} = \frac{\pi^2 N(kT)^2}{4\varepsilon_F} \qquad \text{(Eq. 45)}$$

$$= \frac{\pi^2(6{\cdot}022\times10^{23}\ \text{mol}^{-1})(1{\cdot}38\times10^{-23}\ \text{J K}^{-1})^2(298\,\text{K})^2}{4(5{\cdot}04\times10^{-19}\,\text{J})} = \mathbf{49{\cdot}9\ J\ mol^{-1}}$$

Notice that the electronic contribution to thermal energy in Na metal at room temperature is far greater than the Fermi energy of the metal.

Example 23. Calculate the fermi energy of silver metal, given that the atomic mass of silver is 107·868 g mol^{-1}, the density of the metal is 10·5 g cm^{-3}.

Solution : $\rho = 10{\cdot}5 \text{ g cm}^{-3} = 10{\cdot}5\times10^3 \text{ kg m}^{-3}$

$$\therefore \quad V = \frac{M}{\rho} = \frac{107{\cdot}868\times10^{-3}\,\text{kg mol}^{-1}}{10{\cdot}5\times10^3\,\text{kg m}^{-3}} = 1{\cdot}03\times10^{-5}\ \text{m}^3\ \text{mol}^{-1}$$

Since one atom of Ag contains one valence electron, therefore, the number of valence electrons per mole of the metal is $N=6{\cdot}022\times10^{23}$. Thus,

$$\varepsilon_F = \frac{h^2}{8m_e}\left(\frac{3N}{\pi V}\right)^{2/3} = \frac{(6{\cdot}626\times10^{-34}\,\text{J s})^2}{8(9{\cdot}107\times10^{-31}\,\text{kg})}\left[\frac{3(6{\cdot}022\times10^{23}\,\text{mol}^{-1})}{\pi(1{\cdot}03\times10^{-5})\text{m}^3\,\text{mol}^{-1}}\right]^{2/3} = \mathbf{8{\cdot}80\times10^{-19}\ J}$$

Band Theory of Solids. The band theory of solids aims at explaining vast differences in the conductivity of metals which the wave mechanical free electron theory failed to do. This theory was first formulated by F. Bloch (of NMR fame, best known for the Bloch equations in NMR), begins with the Schrödinger wave equation and incorporates the *periodic* potential energy $V(x)$ of a lattice of atoms. The equation thus obtained, called the **Bloch equation,** is written as

$$-\frac{\hbar^2}{2m_e}\frac{d^2\psi}{dx^2} + V(x) = E\psi \qquad \text{...(46)}$$

Since the potential energy is periodic, $V(x) = V(x+na)$ where a is the repeat distance along the x direction in the lattice and n is an integer. Bloch gave the solution of Eq. 46 as

$$\psi_k(x) = u_k(x)\exp(ikx) \qquad \text{...(47)}$$

where $u_k(x)$ is an eigenfunction with the periodicity a of the lattice. A one-electron wave function of the form (47) is called a **Bloch function** and can be decomposed into a sum of *travelling waves.* Bloch functions can be assembled into *localized wave packets* to represent electrons that propagate freely through the periodic potential field of the ion cores. The dependence of the energy on k is quadratic ($E_k = \hbar^2k^2/2m_e$), as in the free-electron theory. However, for $k = \pm n\pi/a$, discontinuities appear in energy that lead to a band structure (Fig. 31).

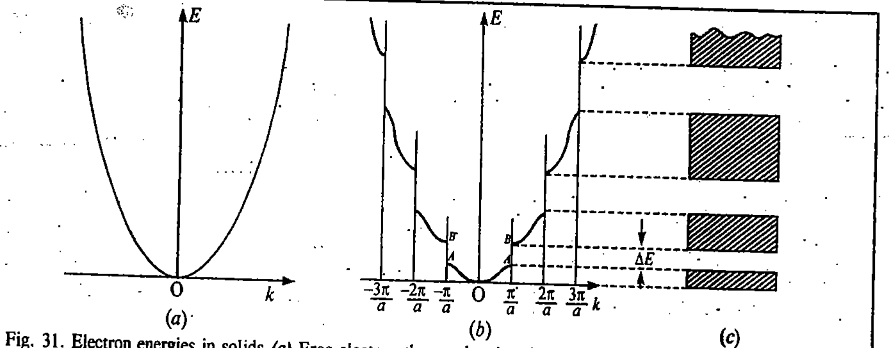

Fig. 31. Electron energies in solids *(a)* Free-electron theory showing the quadratic dependence of E on k ($k\hbar$ is the quasi-momentum of the electron). *(b)* Energy bands showing gaps ΔE at values of k for which the Bragg equation holds. The positions A and B correspond to waves ψ_1 (cos $(\pi x/a)$) and ψ_2 (sin $(\pi x/a)$), respectively ; the values of k ($\pm n\pi/a$) define the boundaries of the one-dimensional Brillouin zones. *(c)* Structure of quasi-continuous energy bands separated by gaps ΔE_i (i = 1, 2, ...).

The space in which k is measured is generally called **k-space.** It is the reciprocal space of X-ray crystallography but whereas crystallography is concerned with the (weighted) reciprocal lattice points, k-space is the *entire* space under investigation. As expected, k has the dimensions of reciprocal length. Each energy state specified by k or by n_x, n_y and n_z, can accommodate two electrons with spins ±1/2 and can be regarded as a point in k-space. [For a cubic crystal, $k = i(k_x + k_y + k_z) = i(\pi/a)(n_x + n_y + n_z)$].

The surface of constant energy E_F in k-space is called the **Fermi surface** ; it separates filled orbitals from unfilled orbitals.

For most values of k, the electrons behave very much like free electrons. However, at values of k = equal to $\pm n\pi/a$, the condition for Bragg reflection of electron waves in one dimension is realized : $k = \pm n\pi/a$ is equivalent to the Bragg equation $2a \sin\theta = n\lambda$ where $k = 2\pi/\lambda$ and $\sin\theta = 1$. The first order reflection at $k = \pm n\pi/a$ arises because waves reflected from adjacent atoms interfere constructively, the phase difference being 2π. The region lying between $\pm \pi/a$ is called the first **Brillouin zone** (Fig. 32). The energy is quasi-continuous within a zone because the energy levels are very closely spaced in a solid but discontinuous at the zone boundaries. As k increases towards $n\pi/a$, the eigenfunctions (6) contain increasing amounts of Bragg-reflected wave. At $k = \pi/a$, for example, the wave $\exp(i\pi x/a)$ reflects as $\exp(-i\pi x/a)$ and the resulting combinations are *standing waves* ψ_1 and ψ_2 of the forms $\cos(\pi x/a)$ and sin $(\pi x/a)$, respectively. Brillouin zones are not normally encountered in X-ray crystal structure analysis but they are essential to an analysis of electron energy levels in solids.

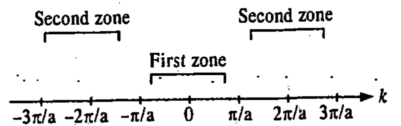

Fig. 32. Boundaries for the first two Brillouin zones in a one-dimensional lattice of periodicity *a*.

The probability densities of the two standing waves are $|\psi_1{}^2|$ and $|\psi_2|^2$, whereas that for the *travelling wave* is exp $(i2kx)$.

Fig. 33. Illustrates a one-dimensional periodic potential field and the wave probability functions described above. The travelling wave distributes charge uniformly along the x-axis ; ψ_1 has its peaks at na and ψ_2 has its peaks at $(n+1/2)a$. The potential energies of the two distributions follow the order $|\psi_1|^2 < \exp(i2kx) < |\psi_2|^2$. Hence, an energy gap ΔE arises and the waves ψ_1 and ψ_2 correspond to the points A and B in Fig. 31. The combination of the waves $\exp(\pm ikx)$ at $k = \pm n\pi/a$, *i.e.*, at the boundaries of the Brillouin zones leads to an energy gap ΔE of $2V_k$ where V_k is the potential energy function at the position in k-space corresponding to k. This result may be compared with the bonding/antibonding situation in MOT (molecular orbital theory) which also depends on a core potential energy.

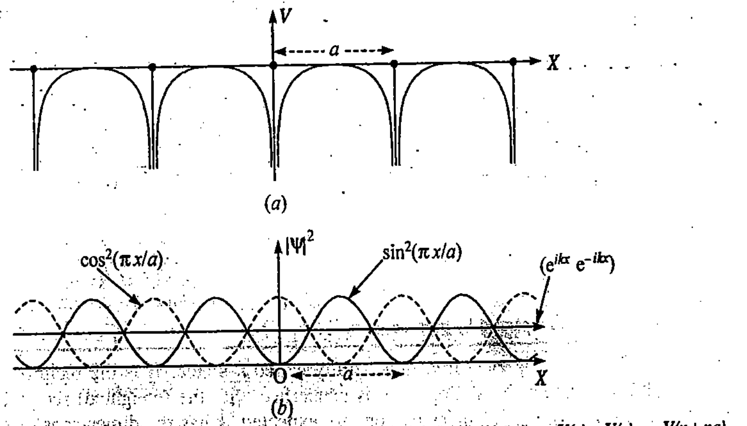

Fig. 33. One-dimensional function with lattice periodicity *a*. *(a)* Periodic potential energy $V(x)$; $V(x) = V(x+na)$. *(b)* Probability densities $\cos^2(\pi x/a)$, $\sin^2(\pi x/a)$ and $[\exp(ikx)\exp(-ikx)]$.

Brillouin zones may be extended to two and three dimensions. The zone boundaries are determined by the regions in k-space where the Bragg equation is satisfied : they are governed by crystal structure rather than by chemical composition.

The first Brillouin zone is the smallest volume in k-space that is entirely enclosed by planes that are normal to and bisect the shortest reciprocal lattice vectors drawn from the origin of k-space. The Brillouin zones correspond to Wigner-Seitz cells in k-space. The **Wigner-Seitz cell** for the lattice based on a conventional primitive cubic unit cell is, itself, a cube ; for the lattice based on the conventional face-centered cubic unit cell, it is a rhombic dodecahedron.

A Wigner-Seitz cell is obtained by joining a point of the Bravais lattice to all the nearest lattice points and then bisecting these lines with perpendicular planes. (The same construction is encountered with Voronoi polyhedra). The intersections of these planes contain the Wigner-Seitz cell. The planes of larger areas are those which are closer to the origin point ; beyond a certain distance, lattice points will not contribute to a Wigner-Seitz cell because the bisecting planes lie outside the confines of the smallest polyhedron. Wigner-Seitz cells are unit cells in the sense that they stack to fill space completely.

Energy Band Theory of Conductors, Semiconductors and Insulators

The basic difference between conductors, semiconductors and insulators lies in the number of *free electrons* present in the material. This difference can be best understood on the basis of the band theory of solids. We know that the energy levels of electrons in an atom are quantized. When an array of several atoms is considered, as is the case in a metallic solid where the atoms occupy the lattice sites, the energy levels of electrons form a series which can be grouped into **bands**, as shown in Fig. 34.

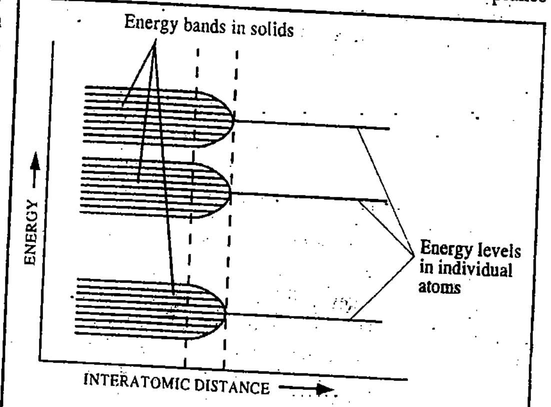

Fig. 34. Formation of energy bands in a solid.

The difference of energy between the energy levels within a band is very small compared with the **energy gap** between the bands. The energy band diagrams of a conductor, an insulator and a semi-conductor are given in Fig. 35.

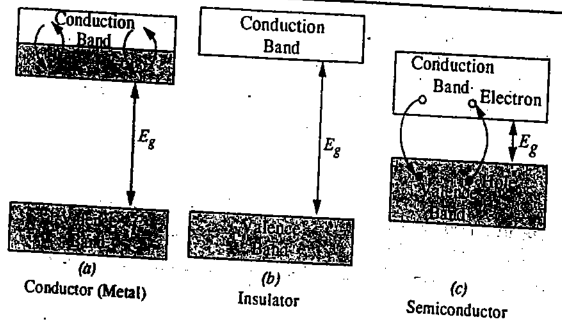

Fig. 35. Energy band diagrams of *(a)* conductor, *(b)* insulator *(c)* semiconductor

Conductors. In a conductor (such as a metal), the valence band (V.B.) is full of electrons while the conduction band (C.B.) is only partly filled. Only a small amount of energy suffices to allow electrons to move within the conduction band, some rising to a higher energy level and others returning to a lower energy level. This movement of electrons within the C.B. constitutes electrical conduction. In some metallic conductors, the V.B. and the C.B. actually overlap resulting in a partly filled top band. The diference in energy between the V.B. and the C.B. is called the energy gap, E_g.

Insulators. In an insulator, the V.B. is full and the E_g is very large. Thus, it will take a great deal of energy to make an electron jump the energy gap and to cause the insulator to break down. The break-down does not occur even at very high temperatures or under very large electric fields. Rubber is an example of an insulator.

Semiconductors. We shall deal with the so-called **intrinsic semiconductor** which is a semiconductor in 'its own right', *i.e.*, no impurity has been added to it. The best known intrinsic semiconductors are silicon and germanium. In an intrinsic semiconductor, the V.B. is full and the C.B. is empty at very low temperatures. The E_g between the two bands is, however, so small that electrons can jump across it by the addition of a small amount of thermal energy (k_B/T) alone, *i.e.*, only heating the material results in electrical conduction. The electrical conductivity increases with increase in temperature since more and more electrons are liberated with increase in temperature. The smaller the value of E_g, the better the semiconductor. Thus, germanium (E_g=0·67 eV) is a better conductor than silicon (E_g=1·14 eV). As an electron jumps from the V.B. to the C.B., it leaves behind a **hole** in the V.B. The hole is positively charged and since an electron can jump into the hole from another part of V.B., it is as if the hole was moving ! Conduction can occur either by the negative electrons moving within the C.B. or by positive holes moving within the V.B.

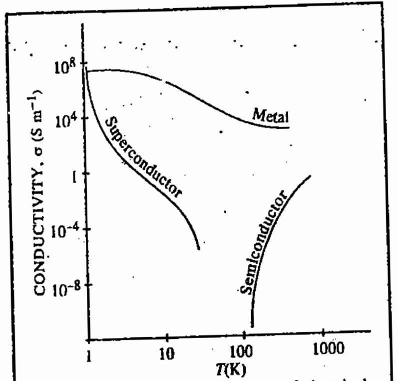

Fig. 36. Temperature-dependence of electrical conductivity of a metal, a semiconductor and a superconductor.

A semiconductor at room temperature generally has much lower conductivity than a metallic conductor because only very few electrons and holes can act as charge carriers. The temperature-dependence of electrical conductivity, σ, for a metallic conductor, a semiconductor and a superconductor is shown in Fig. 36. A super conductor is one which has zero or very little electrical resistance.

As can be seen, a **metallic conductor** is a substance with electrical conductivity that decreases with increasing temperature, a **semiconductor** is a substance with an electrical conductivity that increases with increasing temperature and a **superconductor** is a substance that has zero electrical resistance below a certain temperature called critical temperature.

The conductivity of a semiconductor follows the Arrhenius type temperature-dependence with activation energy, E_a, approximately equal to half of the energy gap, E_g. Thus,

$$\sigma = \sigma_0 \exp(-E_a/kT) = \sigma_0 \exp(-E_g/2kT)$$

The E_g and σ values for the elements of Group IV are given in Table 8.

TABLE 8

Electrical Conductivities and Energy Gaps for the Elements of Group IV

Element	E_g (eV)	σ (S m⁻¹)
C (diamond)	6·0	$< 10^{-4}$
Si	1·14	$1·5\times10^{-3}$
Ge	0·67	2
Sn (gray)	0·08	> 100

Extrinsic Semiconductors

It is possible to increase the charge carriers if atoms with more electrons than the parent element can be introduced by the process known as **doping**. Extremely low concentrations of the dopant (about one atom per 10^9 atoms of the host material) are needed. Pure silicon (Si) and germanium (Ge) can be made more conducting in a controlled manner by adding dopant impurities which act as charge carriers. Si or Ge are first made extremely pure by zone refining. Then some arsenic (As) atoms with five valence electrons are added to the Ge crystal. An extremely small number of Ge atoms are randomly replaced by As atoms. Only four of the five outer electrons on each As atom are required to form bonds in the lattice. The fifth electron on As atom is not bonded. At low temperatures, the fifth electron is localized on the As atom. However, at normal temperatures, some of these fifth electrons on As are excited into the conduction band where they act as charge carriers. This produces what is known as **extrinsic conduction.** Since the current is carried by excess electrons, this is known as ***n*-type semiconduction.** The magnitude of semiconductivity in an extrinsic semiconductor is far greater than that in an intrinsic pure semiconductor.

If the donor As atoms are far apart from one another, their electrons are localised and the **donor band** will be narrow (Fig. 37*a*). The filled dopant band lies near (just below) the empty conduction band of the lattice.

Alternatively, a crystal of pure Si or Ge is doped with atoms of an element which has three valence electrons per atom, such as gallium (Ga) or indium (In). Each gallium atom has three outer electrons to form three bonds in the lattice, these electrons cannot form four bonds in the lattice to complete the covalent structure. One bond is incomplete and the site which remains unoccupied because of the missing electron is called a **positive hole.** More formally, the dopant atoms form a very narrow empty **acceptor band** that lies above the full silicon valence band (Fig. 37*b*). At T=0 K, the acceptor band is empty but at $T > 0$ K, it can accept thermally excited electrons from the Si valence band. This forms new positive holes in the Si valence band. The holes appear to move in a direction opposite to the motion of electrons. The positive holes 'hop' through the band. Since the charge carriers are now the positive holes, this type of conduction is known as ***p*-type conduction.** In principle, any of the Group V elements (such as P, As, Sb, Bi) can be used to make *n*-type semiconductors but, because of its low melting point, As is most commonly used. Similarly, any of the Group III elements (such as B, Al, Ga and In) can be used to make *p*-type semiconductors, though indium (In) is most commonly used because of its low melting point. A minute amount of donor impurity can produce a dramatic change in the conductivity of a semicondcutor. For example, 1 part of a donor impurity per 10^9 parts of germanium increases its conductivity by a factor of 10^3.

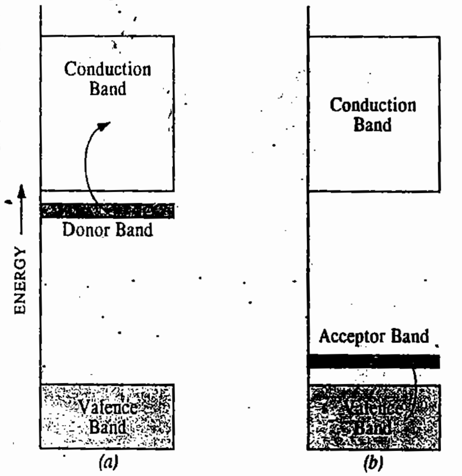

Fig. 37. The band structure of *(a)* an *n*-type semiconductor *(b)* a *p*-type semiconductor.

The combination of *n* and *p*-type semi-conductors (known as ***n–p* junction**), finds interesting applications in the manufacture of **transistors.** This device can conduct electric current more easily in one particular direction than in the reverse direction and, therefore, can be used as a **rectifier** for changing alternating current into direct current. The device is schematically represented in Fig. 38.

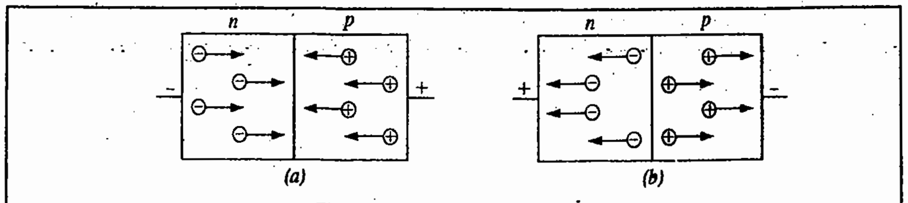

Fig. 38. Semiconductor acting as rectifier.

The material on the left side of each junction is n–type conductor obtained by doping germanium with, say, arsenic. The minus signs represent extra electrons. The material on the right side of the junction is p–type conductor obtained by doping germanium with, say, indium. The positive signs represent 'positive holes' arising from the deficiency of electrons at the indium impurity centres. When an external voltage is applied in such a way as to cause motion of electrons (n–current) from left to right and motion of positive holes (p–current) from right to left (Fig. 35a), current is readily conducted. If direction of voltage is reversed so that there is separation of electrons and positive holes as shown in Fig. 35(b), there is cancellation of n and p–currents and hence the conduction stops. Thus, the n–p junction permits the current from an out side source to flow in one direction only.

Superconductivity

Superconductivity or superconduction is of two types, *viz.*, low temperature superconductivity (LTSC) and high temperature superconductivity (HTSC). An ideal superconductor is supposed to have zero or very little electrical resistance.

Low Temperature Superconductivity (LTSC). LTSC was first discovered in 1911 by the Dutch physicist H. Kamerlingh-Onnes who was awarded the 1913 Physics Nobel Prize for his contributions to low temperature physics which led to the production of liquid helium. He found that down to 4·15 K, the resistance of mercury decreased with decrease in temperature as is the case with most metals. However, at critical temperature T_c=4·15 K, the resistance fell sharply close to zero. Thus, at or below the critical temperature, mercury became a **superconductor**. At very low temperatures, many metals, alloys and certain compounds become superconductors, the critical temperatures for superconductivity lying between 0·1 K and 10 K. Since a superconductor has almost zero resistance, it can carry an electric current without losing energy and, in principle, the current can flow for ever. Superconductors also exhibit what is called **Meissner effect :** it states that a superconductor does not allow the magnetic field to pass through it. In other words, it behaves like a perfectly **diamagnetic substance**. The Meissner effect gives rise to **levitation**; levitation occurs when objects float in air. This can be achieved by the mutual repulsion between a permanent magnet and a superconductor. A superconductor is diamagnetic because it expels all internal magnetic fields arising from unpaired electrons. The key to understanding LTSC was provided by the celebrated **BCS theory** proposed in 1957 by the American physicists J. Bardeen, L. Cooper and J. Schreifer who were awarded the 1972 Physics Nobel Prize. The central role in the BCS theory of LTSC is played by the **Cooper pair**. L. Cooper explained how two electrons could interact in a superconductor forming a *'bound state'* despite their coulombic repulsion. The Cooper pair of electrons exist on account of the indirect interaction of the two electrons via the nuclei of the atoms in the lattice. The lattice is slightly *deformed* as an electron moves through it, with the positive ions in the path of the electrons being displaced towards it. The deformation produces a region of increased positive charge. Another electron passing through this polarized region will be attracted by the greater concentration of the positive charge there. If the attraction is stronger than the repulsion between the electrons, the electrons are effectively coupled together into a Cooper pair with the deformed lattice as the intermediary.

A Cooper pair undergoes less scattering than an individual electron as it travels through the lattice because the distortion caused by one electron can attract back the other electron should it be scattered out of its path in a collision. Since the Cooper pair is stable against scattering, it can carry charge freely through the solid thereby giving rise to superconduction. The BCS theory, which is a mathematical *tour de force*, shows that the two electrons of the Cooper pair must be moving in opposite directions and their correlations may persist over lengths as large as 10^{-6} m. The binding energy of the Cooper pair is of the order of 10^{-3} eV. That is why superconductivity is a low–temperature phenomenon. When $h\nu >>$ binding energy, strong absorption occurs as the Cooper pairs break down. The binding energy at 0 K, $E_g(0)$, is given by

$$E_g(0) = 3{\cdot}53\ kT_c \qquad ...(48)$$

Eq. 48 shows good agreement with the observed values of E_g and T_c. At $T > 0$ K, only a few of the Cooper pairs break down. The resulting individual electrons interact with the remaining Cooper pairs and reduce E_g. Finally, at T_c, E_g disappears ; there are no more Cooper pairs and the material ceases to be a superconductor.

It may be mentioned that since the electrons in a Cooper pair have opposite spins, the pair has resultant zero spin. Thus, the electron pairs in a superconductor are bosons (unlike individual electrons with spin $\frac{1}{2}$ which are fermions) and any number of them can exist in the same quantum state at the same time. Also, the current in a superconductor involves the entire system of Cooper pairs acting as a unit.

We may mention here that the American physicist John Bardeen (1908-1991) was the only physicist to win two Nobel Prizes in physics. He had shared the first Nobel Prize in 1956 with Walter Brattain (1902-1987) and William Shockley (1910-1989) for their researches on semiconductors and their discovery of the transistor effect.

High Temperature Superconductivity (HTSC). Because of the very low temperatures at which most materials become superconducting which implies that T_c is very low, LTSC has not found widespread use. The highest value of T_c known until 1986 was about 23 K. In that year, G. Bednorz and A. Muller (who were working for IBM in Zurich; Switzerland) discovered a cuprate, *viz.*, a mixed oxide Ba–La–Cu–O system, which had a T_c of about 35 K. Bednorz and Muller were awarded the 1987 Physics Nobel Prize for the discovery of HTSC. Another high T_c superconductor $YBa_2Cu_3O_{7-x}$ ($x \lesssim 0{\cdot}1$) was discovered in 1987 by Chinese–American physicists, Wu, Chu and their coworkers, the T_c being 93 K. This temperature is significant because it allows liquid nitrogen (boiling point 77 K) to be used as a coolant rather than the more expensive liquid helium. This superconductor, called yttrium–barium–cuprate, is the 1–2–3 system because of the ratio of the metals present. The non–stoichiometry appears to be necessary for HTSC. It appears that copper is necessary for superconductivity since efforts to replace it by other elements have not borne fruit. This cuprate has the **perovskite structure**. This comprises of three cubic perovskite units stacked one on top of the other giving an elongated (tetragonal) unit cell.

Cu Ba O_3
Cu Y O_3
Cu Ba O_3

The upper and the lower cubes have a Ba^{2+} ion at the body–centred position and the smaller Cu^{2+} ion at each corner. The middle cube is similar but has a Y^{3+} ion at the body centre. A perovskite structure has the formula ABO_3 and the stoichiometry of this compound would be $YBa_2Cu_3O_9$. Since the formula actually found is $YBa_2Cu_3O_{7-x}$, there is evidently a massive oxygen deficiency ; about 25% of oxygen sites in the crystal are vacant.

The LTSC of metals and alloys has been explained by the BCS theory. However, there is at present no satisfactory theory of HTSC. Nevertheless, the following features may be borne in mind :

1. Many warm superconductors contain copper which is known to exist in three oxidation states, (+I), (+II) and (+III). Also Cu(II) forms many tetragonally distorted complexes.

2. The high T_c superconductors are related to the perovskite structure.

3. The oxygen deficiency is very important. Neutron diffraction studies reveal that the vacancies left by the missing O atoms are well ordered. Since Cu is normally octahedrally surrounded by six O atoms, when an O vacancy occurs, the two Cu atoms may interact directly with each other. Interactions such as Cu^{II}–Cu^{III} or Cu^{I}–Cu^{II} may occur by the transfer of an electron between the two Cu atoms. Similarly, HTSC of $YBa_2Cu_3O_{7-x}$ is believed to occur by the ready transfer of electron between Cu(I), Cu(II) and Cu(III).

The preparation of warm superconductors is an art involving grinding, heating, annealing or slow cooling, etc. The '1–2–3' superconductor (yttrium barium cuprate) can be prepared by the *p*H–adjusted precipitation and high–temperature decomposition of the carbonates :

$$2Y^{3+} + 3HCO_3^- \xrightarrow{-H^+} Y_2(CO_3)_3\downarrow$$

$$Ba^{2+} + HCO_3^- \xrightarrow{-H^+} BaCO_3\downarrow$$

$$Cu^{2+} + HCO_3^- \xrightarrow{-H^+} CuCO_3\downarrow$$

$$Y_2(CO_3)_3 + 4BaCO_3 + 6CuCO_3 \xrightarrow{950°C} 2YBa_2Cu_3O_{7-x} + 13CO_2\uparrow$$

IMPERFECTIONS IN A CRYSTAL

The discovery of imperfections in an otherwise ideally perfect crystal is one of the most fascinating aspects of solid state science. An ideally perfect crystal is one which has the same unit cell and contains the same lattice points throughout the crystal. The term **imperfection** or **defect** is generally used to describe any deviation of the ideally perfect crystal from the **periodic** arrangement of its constitutents. Two types of defects are generally observed in crystals. These are : 1. Point Defects 2. Line Defects.

Point Defects

If the deviation occurs because of missing atoms, displaced atoms or extra atoms, the imperfection is named as a **point defect.** Such defects can be the result of imperfect packing during the original crystallisation or they may arise from thermal vibrations of atoms at elevated temperatures because with increase in thermal energy there is increased probability of individual atoms jumping out of their positions of lowest energy. The most common point defects are the Schottky defect and the Frenkel defect. Comparatively less common point defects are the *metal excess defect* and the *metal deficiency defects*. All these defects have been discussed below in some details.

Schottky Defects. These defects arise if some of the lattice points in a crystal are unoccupied. The points which are unoccupied are called *lattice vacancies*. The existence of two vacancies, one due to a missing Na^+ ion and the other due to a missing Cl^- ion in a crystal of NaCl, is shown in Fig. 39. The crystal, as a whole, remains netural because the number of missing positive and negative ions is the same.

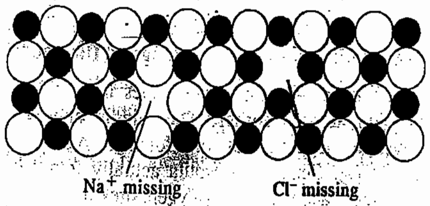

Fig. 39. Schottky defects in a crystal of NaCl.

Schottky defects appear generally in ionic crystals in which the positive and the negative ions do not differ much in size. Sodium chloride and cesium chloride furnish good examples of ionic crystals in which Schottky defects occur.

Because of Schottky defects, the crystal is in a position to conduct electricity to a small extent by an ionic mechanism. It happens as follows : As an electric field is applied, a nearby ion moves from its lattice site to occupy a vacancy. This results in creating a new vacancy and another nearby ion moves into it, and so on. This process continues resulting in the migration of the vacancy and thereby of the ion from one end to the other end of the crystal. In this way, electricity gets conducted across the whole of the crystal.

The existence of vacancies also enables easy movement of atoms or ions in the crystal changing places with one another. *This accounts for the phenomenon of diffusion in solids.*

Number of Schottky defects. Consider an ionic crystal containing N ions in which n Schottky defects are produced by the removal of n cations and n anions from the interior of the crystal. The different ways in which each kind of ion can be removed is given by

$$\frac{N(N-1)(N-2)\ldots(N-n+1)}{n!} = \frac{N!}{(N-n)\,n!} \qquad \text{...(49)}$$

The different ways in which n Schottky defects can be produced is obtained by squaring the expression in Eq. 44 because the number of cation and anion vacancies is equal. Creation of defects in a crystal means creation of disorder. Since entropy is a measure of the disorder of the system, with the creation of defects there is increase in the entropy of the crystal. The entropy S is related to thermodynamic probability W by the Boltzmann equation, *viz.*, $S = k \ln W$, where k is the Boltzmann constant. In the present case, evidently,

$$W = \left(\frac{N!}{(N-n)!\,n!}\right)^2 \qquad \text{...(50)}$$

The increase in entropy causes a change in the Helmholtz free energy. If ε is the enrgy required to create a Schottky defect, then $n\varepsilon$ would be the energy required to create n Schottky defects. Let this energy be designated as E. The Helmholtz free energy is given by $A = E - TS$.

$$\Delta A = \Delta E - T\Delta S = \Delta E - T(S - S_0) = E - TS \qquad \text{(Entropy at 0 K = 0)}$$

$$= E - T\,(k \ln W) = E - kT \ln \left(\frac{N!}{(N-n)!\,n!}\right)^2 \qquad \text{...(51)}$$

Using the Stirling approximation, *viz.*, $\ln x! = x \ln x - x$, for evaluating factorial terms, we find that

$$\ln \left(\frac{N!}{(N-n)!\,n!}\right)^2 = 2\,[\ln N! - \ln (N-n)! - \ln n\,!]$$

$$= 2\,[N \ln N - N - (N-n) \ln (N-n) + (N-n) - n \ln n + n]$$

$$= 2\,[N \ln N - (N-n) \ln (N-n) - n \ln n] \qquad \text{...(52)}$$

Hence, $$\Delta A = E - 2kT\,[N \ln N - (N-n) \ln (N-n) - n \ln n] \qquad \text{...(53)}$$

At equilibrium, at a given temperature, $(\partial(\Delta A)/\partial n)_T = 0$. Also, since N is constant, $\partial N/\partial n)_T = 0$. Hence, from Eq. 52,

$$\left(\frac{\partial(\Delta A)}{\partial n}\right)_T = E - 2\,kT \ln \frac{N-n}{n} = 0 \qquad \text{...(54)}$$

$$\therefore \quad E = 2\,kT \ln\,[(N-n)/n] \qquad \text{...(55)}$$

or $$(N-n)/n = \exp\,(E/2kT) \qquad \text{...(56)}$$

Since the number of Schottky defects, n, is much smaller than the number of ions, N, in a crystal, *i.e.*, $n << N$, hence $N - n = N$. Eq. 55, may thus be written as

$$n = N \exp(-E/2kT) \qquad ...(57)$$

Eq. 56 gives the number of Schottky defects in a crystal.

We may consider a specific example. In NaCl crystal, E is known to be approximately 2eV. Accordingly, the number of Schottky defects present in the NaCl crystal at room temperature comes out to be 10^6 per cm^3. Since the number of the Na^+ and Cl^- ions is approximately 10^{22} per cm^3, we find that, on an average, there is one Schottky defect for 10^{16} ions. Thus, the application of the Stirling approximation in the above derivation is perfectly justified.

Frenkel Defects. These defects arise when *an ion occupies an interstitial position between the lattice points*. This is shown in Fig. 40 for the crystal of AgBr.

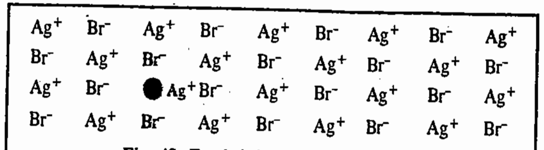

Ag^+ Br^- Ag^+ Br^- Ag^+ Br^- Ag^+ Br^- Ag^+
Br^- Ag^+ Br^- Ag^+ Br^- Ag^+ Br^- Ag^+ Br^-
Ag^+ Br^- ● Ag^+ Br^- Ag^+ Br^- Ag^+ Br^- Ag^+
Br^- Ag^+ Br^- Ag^+ Br^- Ag^+ Br^- Ag^+ Br^-

Fig. 40. Frenkel defects in a crystal of AgBr.

As can be seen, one of the Ag^+ ions occupies a position in the interstitial space rather than its own appropriate site in the lattice. A vacancy is thus created in the lattice as shown. It may be noted again that the crystal remains neutral since the number of positive ions is the same as the number of negative ions. The presence of Ag^+ ions in the interstitial space of AgBr crystal is responsible for the formation of a photographic image on exposure of AgBr crystals (*i.e.*, photographic plate) to light.

ZnS is another crystal in which Frenkel defects appear. Zn^{2+} ions are entrapped in the interstitial space leaving vacancies in the lattice.

Frenkel defects appear in crystals in which the negative ions are much larger than the positive ions. Like Schottky defects, the Frenkel defects are also responsible for the conduction of electricity in crystals and also for the phenomenon of diffusion in solids.

Number of Frenkel defects. Consider an ionic crystal having N ions and N_i interstitial spaces in its structure. The number of ways in which n Frenkel defects can be formed is given by

$$n = \frac{N!}{(N-n)!\,n!} \times \frac{N_i!}{(N_i - n)\,n!} \qquad ...(58)$$

Let the energy required to displace an ion from its proper position to an interstitial position be ε. Then the energy required to produce n Frenkel defects would be $n\varepsilon$. Let this energy be designated by E.

Proceeding as before, using the Boltzmann entropy equation, *viz.*, $S = k \ln W$, the Helmholtz free energy equation, *viz.*, $\Delta A = E - T\Delta S$ and the Stirling approximation for evaluating factorial terms, we arrive at the conclusion that

$$n = (NN_i)^{1/2} \exp(-E/2kT) \qquad ...(59)$$

Eq. 57 gives the number of Frenkel defects in a crystal.

It is evident from Eqs. 57 and 58 that the number of Schottky and Frenkel defects would increase exponentially with increase in temperature. It has been observed by X-ray diffraction of NaCl that while at room temperature there is only one Schottky defect for 10^{15} lattice sites, the number increases to 10^6 at 500°C and to 10^{11} at 800°C for the same number of lattice sites.

Example 24. Estimate the mole fractions of Schottky and Frenkel defects in a NaCl crystal at 1000 K. The energies of formation of these defects are 2eV and 3eV, respectively. 1eV = $1{\cdot}602 \times 10^{-19}$ J ; $k = 1{\cdot}38 \times 10^{-23}$ J K^{-1}.

Solution :

Schottky Defects : According to Eq. 52, the mole fraction of Schottky defects is given by

$$n/N = \exp(-E/2kT)$$

$$= \exp\left[\frac{-(2\text{eV})(1{\cdot}602 \times 10^{-10}\,\text{J}\,(\text{eV})^{-1}}{2(1{\cdot}38 \times 10^{-23}\,\text{J}\,\text{K}^{-1})(1000\,\text{K})}\right] = \exp(-11{\cdot}6) = 9{\cdot}17 \times 10^{-6}$$

Frenkel Defects. According to the structure of the unit cell of NaCl crystal, the number of interstitial spaces is twice the number of Na^+ ions present in the unit cell, that is, $N_i = 2N$. The Frenkel defects are formed only by the migration of the smaller Na^+ ion. According to Eq. 54,

$$n = (NN_i)^{1/2} \exp(-E/2kT)$$

Since $N_i = 2N$, hence

$$n/N = 2^{1/2} \exp(-E/2kT) = 2^{1/2} \exp\left[\frac{-(3\text{eV})(1{\cdot}602 \times 10^{-19}\,\text{J}\,(\text{eV})^{-1}}{(2 \times 1{\cdot}38 \times 10^{-23}\,(\text{J}\,\text{K}^{-1})(1000\,\text{K}))}\right] = 3{\cdot}82 \times 10^{-8}$$

Metal Excess Defects. The Colour Centres. It has been observed that if a crystal of NaCl is heated in sodium vapour, it acquires a yellow colour. This yellow colour is due to the formation of a non-stoichiometric compound of sodium chloride in which there is a slight excess of sodium ions. What happens in this case is that some sodium metal gets doped into the sodium chloride crystal each atom of which gets ionised into Na^+ and e^- due to crystal energy. This electron occupies a site that would otherwise be filled by a chloride ion, as illustrated in Fig. 41.

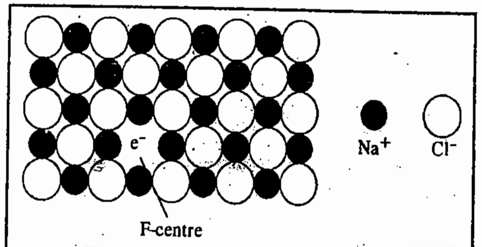

Fig. 41. F-centre in a sodium chloride crystal.

There is evidently an excess of Na^+ ions although the crystal as a whole is neutral. A little reflection would show that there are six Na^+ sites adjacent to the vacant site occupied by the electron. The extra electron is thus shared between all the six Na^+ ions which implies that this electron is *not localised* at the vacant Cl^- site. On the other hand, this electron is similar to the delocalised π electrons present in molecules containing conjugate double bonds. Light is absorbed when this delocalised electron makes an easy transition from its ground state to an excited state. As a result, the non-stoichiometric form of sodium chloride *appears coloured*. Because of this, the sites occupied by the extra electrons are known as **colour centres**. These are also called **F-centres**. This name comes from the German word Farbe meaning *colour*. The non-stoichiometric sodium chloride may be represented by the formula $Na_{(1+\delta)}Cl$ where δ is the excess sodium metal doped in the crystal because of its exposure to sodium vapour.

Another common example of metal excess defects is the formation of *magenta coloured* non-stoichiometric compound of potassium chloride by exposing the crystals of KCl to K metal vapour. The coloured compound contains an excess of K^+ ions, the vacant Cl^- sites being filled by electrons obtained by the ionization of the excess K metal doped into the crystal.

Metal Deficiency Defects. In certain cases, one of the positive ions is missing from its lattice site and the extra negative charge is balanced by some nearby metal ion acquiring two charges instead of one. There is, evidently, *a deficiency of the metal ions* although the crystal as a whole is neutral. This type of defect is generally found amongst the compounds of transition metals which can exhibit variable valency. Crystals of FeO, FeS and NiO show this type of defects. The existence of metal deficiency defects in the crystal of FeO is illustrated in Fig. 42.

Fe^{2+}	O^{2-}	Fe^{2+}	O^{2-}	Fe^{2+}	O^{2-}	Fe^{2+}	O^{2-}	Fe^{2+}	O^{2-}
O^{2-}	Fe^{2+}	O^{2-}	Fe^{2+}	O^{2-}	Fe^{2+}	O^{2-}	Fe^{2+}	O^{2-}	Fe^{2+}
Fe^{2+}	O^{2-}	Fe^{2+}	O^{2-}	Fe^{2+}	O^{2-}	●	O^{2-}	Fe^{2+}	O^{2-}
O^{2-}	Fe^{2+}	O^{2-}	Fe^{2+}	O^{2-}	Fe^{3+}	O^{2-}	Fe^{3+}	O^{2-}	Fe^{2+}
Fe^{2+}	O^{2-}	Fe^{2+}	O^{2-}	Fe^{2+}	O^{2-}	Fe^{2+}	O^{2-}	Fe^{2+}	O^{2-}

Fig. 42. Metal Deficiency defects in a crystal of FeO.

It is evident from the above discussion that all types of point defects result in the creation of vacancies or 'holes' in the lattices of crystals. The presence of holes lowers the density as well as the lattice energy or the stability of the crystals. The presence of too many holes may cause a partial collapse of the lattice.

Line Defects : Dislocations

In addition to the point defects discussed above, another kind of imperfection occurs when the periodicity of the atomic lattice array is interrupted along certain directions in a crystal. Such interruptions occur along rows of a crystal structure and are called **line defects.** The most common type of line defect within a crystal is a **dislocation.** The presence of dislocations results in easy deformation of a crystal under the influence of a shear stress. The common types of dislocations are the *edge dislocations* and the *screw dislocations*. These are described below.

Edge Dislocations. Edge dislocations arise when there is a slight mismatch in the orientation of adjacent parts of the growing crystal resulting in the introduction of an extra row of atoms. The edge of the atomic plane terminates within the crystal instead of passing all the way through. Under the impact of the shear, the dislocation moves across the crystal in such a way that the top half of the crystal is displaced one lattice-distance with respect to the lower half. The motion of an edge dislocation under shear is illustrated in Fig. 43.

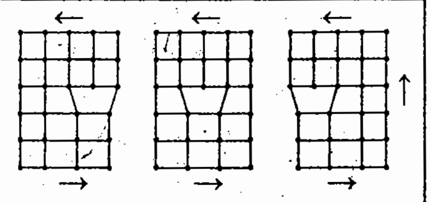

Fig. 43. Motion of an edge dislocation.

Near the edge dislocation, the atoms are pushed together above the edge and pulled apart below the edge. In this way, the impurity atoms with larger diameters than the parent atoms tend to concentrate below the edge and the impurity atoms with smaller diameters tend to concentrate above the edge. As a result of the binding of the impurity at the dislocation, it is more difficult to move a dislocation in an impure material. This is the reason why alloys require greater shear force for permanent deformation than do the pure metals.

Screw Dislocations. The formation of a screw dislocation can be visualised by cutting a rubber stopper parallel to its axis and then pushing on one end so that a jog is created on the other end. If initially the stopper contained atoms at regular lattice points, deformation would convert the parallel planes of atoms normal to the axis into a kind of spiral ramp. Such a displacement of the atoms constitutes what is known as **screw dislocation** (Fig. 44). A screw dislocation helps in easy crystal growth because

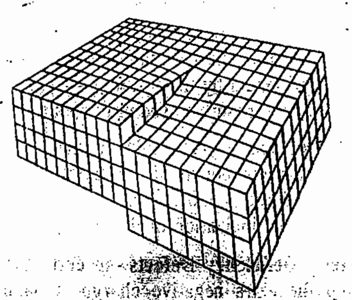

Fig. 44. The formation of a screw dislocation.

atoms can be added at the step. Screw dislocations result in easy deformation of crystal in the same way as is done by edge dislocations. In practice, real dislocations are mixtures of edge dislocations and screw dislocations. Dislocations provide for preferred sites within a crystal for chemical reactions and physical changes (such as phase transformation, precipitation or etching). The point of emergence of a dislocation at the surface of a crystal is a site of enhanced chemical reactivity. The number of dislocations per unit area can be measured by counting the etch pits which are formed at the surface. The number of etch pits formed ranges from 10^5 m^{-2} in the best silver crystal to 10^{15} m^{-2} in a severely deformed crystal.

Imperfections due to Transient Atomic Displacement. The vibrations of a crystal, like those of an S.H.O., have three normal modes of vibration which correspond to one longitudinal mode and two mutually perpendicular transverse modes. When a transition takes place from a higher vibrational to a lower vibrational state, a quantum of thermal energy is emitted. In analogy with a *photon* of radiation energy, the quantum of thermal energy is termed as **phonon.** Absorption of phonons by a crystal can produce atomic displacement leading to imperfections. Unlike point defects and line defects, phonons produce atomic displacements that are time-dependent and hence transient, *i.e.*, short-lived. As the phonons flow through a solid, they collide with atoms and also with one another and are scattered. Energy and momentum are conserved in the scattering process. In addition to phonon-atom and phonon-phonon interactions, there can also be phonon-electron interactions in the crystal. If in a phonon-electron interaction, the electron is raised to an excited state, this would result in the formation of 'holes' in the empty energy state. The excited electron may interact with the hole to form what is called an **exciton**. Thus, all kinds of fascinating phenomena can occur in the crystal lattice as a result of such dynamic interactions. No wonder that solid state physics is, next to elementary particle physics, the most exciting area of scientific research.

The spectacular applications of solid state science have been in materials science, nanotechnology and computers. The 2007 physics Nobel Prize was awarded to the German physicist Peter Gruenberg and the French physicist Albert Fert for their independent discovery of **Giant Magnetoresistance** (GMR). The GMR effect has revolutionized techniques for retrieving data from hard disks in computers, making it possible to miniaturize hard disks radically. Also, another triumph for research in the solid state is the 2009 Physics Nobel Prize for achievements that have helped lay the foundation for the Information Technology (IT) revolution and modern network societies. Charles K. Kao was honoured for achievements concerning the transmission of light in fibres for optical communicaiton and Willard S. Boyle and George E. Smith were honoured for the invention of an imaging semiconductor circuit—the **charge-coupled device (CCD) sensor.**

Quasicrystals

Researchers discovered in 1984 that a rapidly cooled alloy of composition $Al_{86}Mn_{14}$ gave a pattern of discrete spots by electron diffraction that showed the **icosahedral symmetry** $m\bar{5}m$. It follows that, although the structure is not based on a translation unit cell, it has to possess a high degree of three-dimensional regularity in order to exhibit Bragg reflection. Such materials are termed quasicrystals. Fig. 45. shows an icosahedron ; the vertical direction is one of the six $\bar{5}$ axes. An icosahedron may be formed by allowing 20 regular tetrahedra to share a common apex, the central dot in Fig. 45, each tetrahedron distorting slightly in the process.

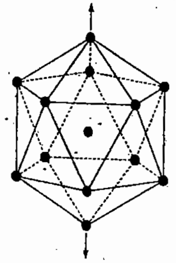

Fig. 45. An icosahedron, point-group symmetry $m\bar{5}m(I_h)$. The polyhedron is centrosymmetric, and the vertical direction is one of the six fivefold inversion axes present.

Other species of icosahedral symmetry are known. For example, the turnip yellow mosaic virus has crystals of point group 532(I). In this case, the inherent icosahedral strain is relieved by incorporating water molecules into the structure. Molecules are known that show five-fold symmetry, as in the metal biscyclopentadienyls $(C_5H_5)M$. For M=Fe, with the cyclopentadienyl rings staggered (Fig. 46), the point group symmetry is $\bar{5}m(D_{5d})$ whereas for M = Ru, with the rings in the eclipsed position, the symmetry is $\overline{10}m2(D_{5h})$.

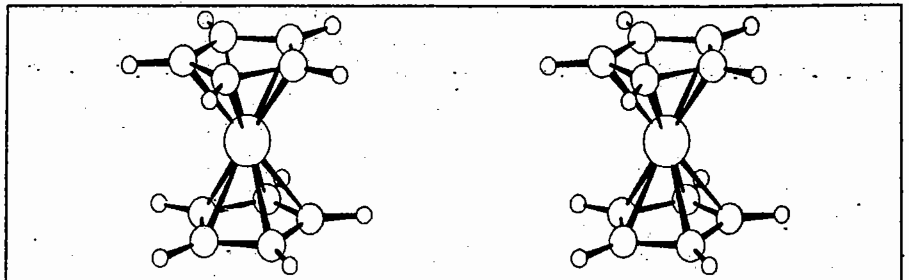

Fig. 46. Stereoview of the molecular structure of biscyclopentadienyl iron, showing the centrosymmetric point-group symmetry $\bar{5}m$ for the molecules ; the two rings are in the staggered position.

A quasicrystal may be considered as a three-dimensional generalization of the two-dimensional **Penrose tiling pattern** (Fig. 47) which consists of rhombi of angles 144° and 108°; the former occurs $(1 + \sqrt{5}) / 2$ times more frequently than the latter ; this number is referred to as the *golden mean* τ. A pentagon of unit side has a diagonal of 2 cos (π/5) or τ, the same value occurs for the distance from the vertex of a regular decagon of unit length sides to its centre. If three rectangular cards with sides in the ratio τ:1 are slotted centrally such that they can be interlinked to form three mutually perpendicular planes, the corners of the card become the vertices of an icosahedron. The value of τ is ... (1·618033989).

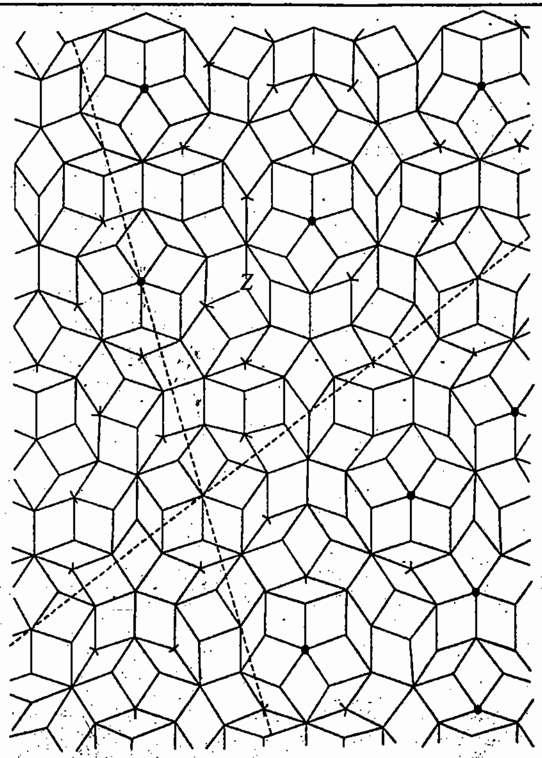

Fig. 47. Two-dimensional Penrose tiling pattern ; the rhombi have angles of 144° and 108°. The similar orientations of the decagons are highlighted by dashed lines at 72° to each other, such lines permeating the whole pattern. It is this type of regularity in three dimensions that enables a quasicrystal to develop Bragg reflections.

Although there is no pure translational symmetry in the tiling pattern, the regular decagons are similarly oriented and lines can be drawn through the corners (atom positions) at 72° (360°/5). In three dimensions, two different rhombohedral cells (compressed cubes) can be packed together to give an icosahedral structure.

For several aspects of the solid state, refer to :

C.N.R. Rao, *Solid State Chemistry : Selected Papers of C.N.R. Rao*, (ed., S.K. Joshi and R.A. Mashelkar), World Scientific, Singapore, 1995.

I. Review Questions

1. Derive the Bragg equation in X-ray crystallography.
2. Discuss how you would use the systematic absences of reflection in the diffraction pattern to distinguish between the three types of cubic Bravais lattices.
3. Derive Born-Lande′ equation for the lattice energy of an ionic solid.
4. Discuss the Fourier synthesis of electron density in a crystal.
5. Describe the Patterson synthesis for determining the relative orientations of pairs of atoms in a crystal.
6. Describe in details the free electron model of metallic structure. Explain how this model accounts for high conductivity of metals. Explain the term Fermi energy.
7. What are extrinsic semiconductors ? Discuss briefly giving diagrams.
8. What are *n*-type and *p*-type semiconductors ? Explain the fabrication of transistors.
9. What is superconductivity ? How would you explain superconductivity of metals.
10. Discuss briefly the following types of defects : *(i)* Schottky defects *(ii)* Frenkel defects *(iii)* Metal excess defects *(iv)* Metal deficiency defects *(v)* Line defects.
11. What are Schottky defects ? Derive an expression for the number of Schottky defects in a crystal.
12. What are Frenkel defects ? Derive an expression for the number of Frenkel defects in a crystal.
13. What are colour centres ? How do they arise ?
14. What are the common types of dislocations ?

II. Problems

1. NaCl has a f.c.c. structure. How many Na^+ and Cl^- ions are there in the unit cell ? **[Ans. Na^+=4, Cl^-=4]**
2. CsCl has a b.c.c. structure. How many Cs^+ and Cl^- ions are there in the unit cell ? **[Ans. Cs^+=1, Cl^-=1]**
3. NaCl crystallises in a face-centred cubic lattice. Calculate the number of unit cells in 1·0 g of the crystal. What is the number along each edge of the crystal ? **[Ans. $2{\cdot}57\times10^{21}$ unit cells, $1{\cdot}37\times10^7$]**
4. Insulin forms crystals of orthorhombic type with unit cell dimensions of 13·0 nm×7·48 nm×3·09 nm. If the density of the crystal is $1{\cdot}315\times10^3$ kg m^{-3} and there are six insulin molecules per unit cell, what is the molar mass of insulin ? **[Ans. 39·7 kg mol^{-1}]**

5. Copper crystallizes in a f.c.c. lattice with the edge length, $a = 360$ pm. If the density of Cu is $8·94 \times 10^3$ kg m^{-3}, calculate the Avogadro's number. (Molar mass of copper = 63·54 g mol^{-1}). **[Ans. $6·095 \times 10^{23}$ mol^{-1}]**

6. Calculate the lattice energy of cesium iodide which crystallizes in the cesium chloride structure and has an interionic distance of 395 pm. The Madelung constant and the Born exponent for CsI are 1·76 and 12, respectively. **[Ans. – 564·8 kJ mol^{-1}]**

7. The only metal that crystallizes in a primitive cubic lattice is polonium which has a unit cell side of 334·5 pm. What are the perpendicular distances between planes with Miller indices (110), (111), (210) and (211) ? **[Ans: 236·5, 193·1, 149·5 and 136·6 pm]**

8. Calculate the interplanar spacing (d_{hkl}) for a cubic system between the following sets of planes : *(a)* 110 *(b)* 111 *(c)* 222. Assume that a is the edge length of the unit cell. **[Ans. *(a)* $d_{110} = a/\sqrt{2}$ *(b)* $d_{111} = a/\sqrt{3}$ *(c)* $d_{222} = a/2\sqrt{3}$]**

9. Calculate the angles at which first, second, and third order reflections are obtained from planes 500 pm apart, using X-rays of wave length 100 pm. **[Ans. 5·74°, 11·54°, 17·46°]**

10. X-rays of wave length 154 pm are diffraction by the 200 plane of AgCl crystal. At what angle would the maximum reflection occur ? Given : $a = 555$ pm. **[Ans. $\theta = 16·1°$]**

11. A powder pattern of MgO, known to crystallize in the cubic system, shows diffraction lines at sin θ values of 0·1461, 0·1690, 0·2801, 0·2801, 0·2935 and 0·3697. Determine the lattice type of MgO. **[Ans. f.c.c.]**

12. NaCl has a face-centred cubic lattice ? What is the coordination number of *(a)* the sodium, and *(b)* the ion ? *(c)* What are the individual lattice structures of sodium and ions in NaCl ? *(d)* What is the number of Na^+ and Cl^- ions in the unit cell of NaCl ? **[Ans. *(a)* 6 *(b)* 6 *(c)* f.c.c., *(d)* $Na^+ = 4$, $Cl = 4$]**

13. A compound alloy of gold and copper crystallizes in a cubic lattice in which gold atoms occupy the lattice points at the corners of a cube and the copper atoms occupy the centres of each of the cube faces. What is the formula of the compound ? **[Ans. $AuCu_3$]**

14. Ag crystallizes in a cubic lattice. The density is $10·7 \times 10^3$ kg m^{-3}. If the edge length of the unit cell is 406 pm, determine the type of the latice. **[Ans. f.c.c.]**

15. Calculate the interplanar spacing (d_{hkl}) for a cubic system between the following sets of planes : *(a)* 110 *(b)* 111 *(c)* 222. Assume that a is the edge length of the unit cell. **[Ans. *(a)* $d_{110} = a/\sqrt{2}$ *(b)* $d_{111} = a/\sqrt{2}$ *(c)* $d_{222} = a/2\sqrt{3}$]**

16. The density of NaCl at 25°C is $2·163 \times 10^3$ kg m^{-3}. When X-rays from a palladium target having a wave length of 58·1 pm are used, the 200 reflection of NaCl occurs at an angle of 5·91°. Calculate the number of Na^+ and Cl^- ions in the unit cell. **[Ans. $n = 3·999 \approx 4$]**

CHAPTER 32

THE COLLOIDAL STATE

The Colloidal Systems. A colloidal dispersion has traditionally been defined as a suspension of small particles in a continuous medium. Because of their ability to scatter light and their very low osmotic pressure, these particles were recognized to be much larger than simple small molecules such as water, alcohol or benzene and simple salts like NaCl. It was assumed that they were aggregates of many small molecules, held together in a kind of amorphous state quite different from the usual crystalline state of these substances. Today we recognize that many of these "aggregates" are in fact single molecules that have a very high molar mass. The size limits are difficult to specify but if the dispersed particles are between 1 μm and 1 nm, we may say that the system is a colloidal dispersion.

There are two classical subdivisions of colloidal systems : (1) *lyophilic* or *solvent-loving* colloids (also called *gels*) and (2) *lyophobic* or *solvent-fearing* colloids (also called *sols*).

The **lyophilic colloids** are invariably polymeric molecules so that the colloidal solution consists of a dispersion of single molecules. The stability of the lyophilic colloid is a consequence of the strong, favourable solvent–solute interactions. Typical lyophilic systems would be proteins (especially gelatin) or starch in water, rubber in benzene and cellulose nitrate or cellulose acetate in acetone. The process of dissolution may be rather slow. The first additions of solvent are slowly absorbed by the solid which swells as a result (this stage is called *imbibition*). Further addition of solvent together with mechanical kneading (as in the case of rubber) slowly distributes the solvent and solute uniformly. In the case of ordinary gelatin, the dissolution process is aided considerably by raising the temperature. As the solution cools, the long and twisted protein molecules get entangled in a network with much open space between the molecules. The presence of the protein induces some structure in the water which is physically trapped in the interstices of the network. The result is a gel. The addition of gross amounts of salts to a hydrophilic gel will ultimately precipitate the protein. However, this is a consequence of competition between the protein and the salt for the solvent, water. Lithium salts are particularly effective because of the large amount of water than can be bound by the lithium ion. The charge of the ion is not a primary determinant of its effectiveness as a precipitant.

The **lyophobic colloids** are invariably substances that are highly insoluble in the dispersion medium. The lyophobic colloids are usually aggregates of small molecules (or in cases where a molecule is not defined, such as AgI, they consist of a large number of units of the formula).

Preparation of Lyophobic Colloidal Solutions

The primary consideration in the preparation of colloidal solutions is that the dispersed particles should be within the size range of 1 mμ–200 mμ. The lyophilic sols can be readily prepared since colloidal materials such as starch, gelatin, acacia, etc., when added to water swell up and spontaneously break into particulates of matter of colloidal range. The lyophobic sols, however, require special techniques for their preparation. The methods consist either in 1. *Breaking down the coarser aggregates into particles of colloidal size* or 2. *Grouping molecules into larger aggregates of colloidal size*. The methods belonging to these two categories are known as **dispersion** and **condensation** methods, respectively.

A. Dispersion Methods. 1. Mechanical Dispersion. The most obvious method of dispersion